US009437372B1

(12) **United States Patent**
Zhamu et al.

(10) **Patent No.:** **US 9,437,372 B1**
(45) **Date of Patent:** **Sep. 6, 2016**

(54) **PROCESS FOR PRODUCING GRAPHENE FOAM SUPERCAPACITOR ELECTRODE**

(71) Applicants: **Aruna Zhamu**, Springboro, OH (US); **Bor Z Jang**, Centerville, OH (US)

(72) Inventors: **Aruna Zhamu**, Springboro, OH (US); **Bor Z Jang**, Centerville, OH (US)

(73) Assignee: **Nanotek Instruments, Inc.**, Dayton, OH (US)

(*) Notice: Subject to any disclaimer, the term of this patent is extended or adjusted under 35 U.S.C. 154(b) by 0 days.

(21) Appl. No.: **14/998,474**

(22) Filed: **Jan. 11, 2016**

(51) **Int. Cl.**
H01G 9/00	(2006.01)
H01G 11/86	(2013.01)
C04B 35/52	(2006.01)
C04B 38/02	(2006.01)
C04B 38/06	(2006.01)
C04B 41/45	(2006.01)
H01G 11/32	(2013.01)
H01G 11/34	(2013.01)
H01G 11/36	(2013.01)
H01G 11/38	(2013.01)

(52) **U.S. Cl.**
CPC *H01G 11/86* (2013.01); *C04B 35/52* (2013.01); *C04B 38/02* (2013.01); *C04B 38/06* (2013.01); *C04B 41/4505* (2013.01); *H01G 9/00* (2013.01); *H01G 11/32* (2013.01); *H01G 11/34* (2013.01); *H01G 11/36* (2013.01); *H01G 11/38* (2013.01)

(58) **Field of Classification Search**
CPC H01G 11/86; H01G 11/32; H01G 11/34; H01G 11/36; H01G 11/38; H01G 9/00; C04B 35/52; C04B 38/02; C04B 38/06; C04B 41/4505
See application file for complete search history.

(56) **References Cited**

U.S. PATENT DOCUMENTS

6,649,538 B1*	11/2003	Cheng	....	H01L 21/28185
				257/E21.268
7,071,258 B1	7/2006	Jang et al.		
7,623,340 B1	11/2009	Song et al.		
8,497,225 B2*	7/2013	Zhamu	....	H01G 11/34
				361/321.4
9,315,388 B2*	4/2016	Burton	....	C01B 31/0469
9,359,208 B2*	6/2016	Zhamu	....	C01B 31/04
9,382,117 B2*	7/2016	Zhamu	....	C01B 31/043
2011/0046027 A1*	2/2011	Zhamu	....	C10M 103/02
				508/113
2016/0019995 A1*	1/2016	Zhamu	....	H01B 1/04
				428/219
2016/0043384 A1*	2/2016	Zhamu	....	H01M 4/133
				429/231.4

OTHER PUBLICATIONS

U.S. Appl. No. 10/858,814, filed Jun. 3, 2004, B. Z. Jang, et al.
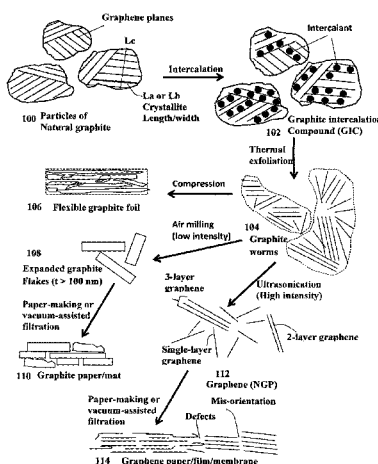(Continued)

Primary Examiner — Savitr Mulpuri

(57) **ABSTRACT**

A process for producing a supercapacitor electrode, comprising: (a) preparing a graphene dispersion containing an optional blowing agent; (b) depositing the dispersion onto a supporting substrate to form a wet layer; (c) removing the liquid medium from the wet layer to form a dried layer of graphene material; (d) heat treating the dried layer at a temperature from 80° C. to 3,200° C. to induce volatile gas molecules from the non-carbon elements or to activate the blowing agent for producing a layer of solid graphene foam having a physical density from 0.01 to 1.7 g/cm³ and a specific surface area from 50 to 3,300 m²/g; and (e) impregnating the foam with an electrolyte to form a layer of pre-impregnated graphene foam, which is compressed to form the electrode. This process leads to a supercapacitor having a large electrode thickness, high active mass loading, high tap density, and exceptional energy density.

21 Claims, 18 Drawing Sheets

(56)   **References Cited**

OTHER PUBLICATIONS

U.S. Appl. No. 11/509,424, filed Aug. 25, 2006, B. Z. Jang, et al.
U.S. Appl. No. 11/906,786, filed Oct. 4, 2007, A. Zhamu, et al.
U.S. Appl. No. 11/895,657, filed Aug. 27, 2007, A. Zhamu, et al.
U.S. Appl. No. 11/895,588, filed Aug. 27, 2007, A. Zhamu, et al.
U.S. Appl. No. 12/220,651, filed Jul. 28, 2008, A. Zhamu, et al.
B. Z. Jang and A Zhamu, "Processing of Nano Graphene Platelets (NGPs) and NGP Nanocomposites: A Review," J. Materials Sci. 43 (2008) 5092-5101.

B. G. Choi, et al., "3D Macroporous Graphene Frameworks for Supercapacitors with High Energy and Power Densities," ACS Nano, 6 (2012) 4020-4028.
Z. Chen, et al., "Three-dimensional flexible and conductive interconnected graphene networks grown by chemical vapour deposition," Nature Materials, 10 (Jun. 2011) 424-428.
Y. Xu, et al. "Self-Assembled Graphene Hydrogel via a One-Step Hydrothermal Process," ACS Nano 2010, 4, 4324-4330.

* cited by examiner

FIG. 1(A)

Graphene planes

Lc

Intercalation

Intercalant

La or Lb
Crystallite
Length/width

100 Particles of
Natural graphite

102 Graphite intercalation
Compound (GIC)

Thermal
exfoliation

Compression

106 Flexible graphite foil

Air milling
(low intensity)

104
Graphite
worms

108

Expanded graphite
Flakes (t > 100 nm)

3-layer
graphene

Ultrasonication
(High intensity)

Paper-making or
vacuum-assisted
filtration

2-layer graphene

Single-layer
graphene

110 Graphite paper/mat

112
Graphene (NGP)

Paper-making or
vacuum-assisted
filtration

Mis-orientation

Defects

114   Graphene paper/film/membrane

FIG. 1(B)

FIG. 2 Prior art

FIG. 3
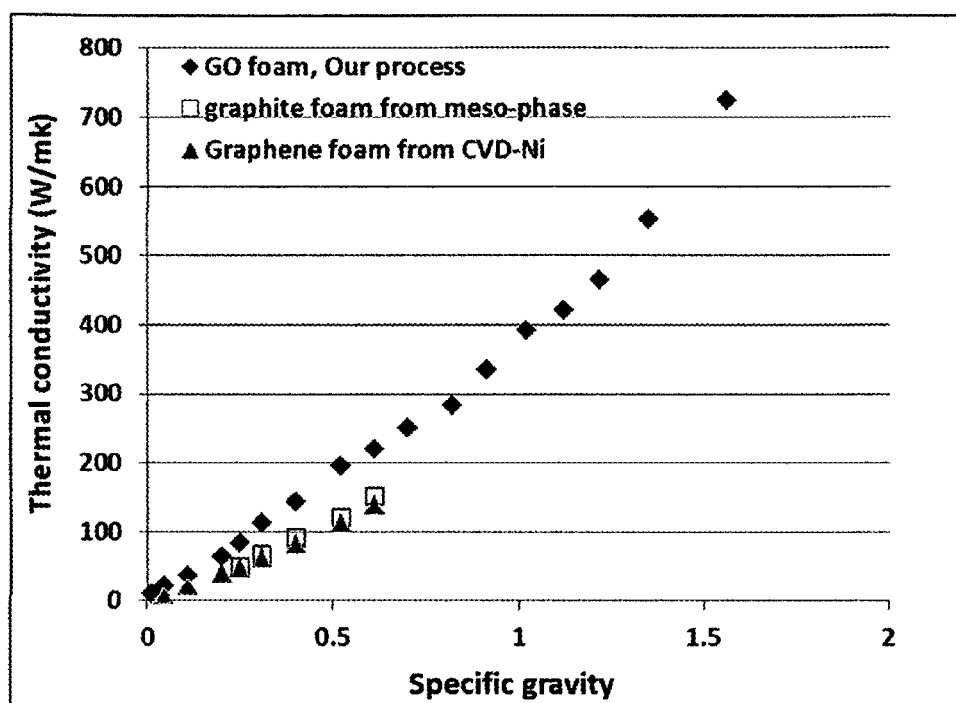
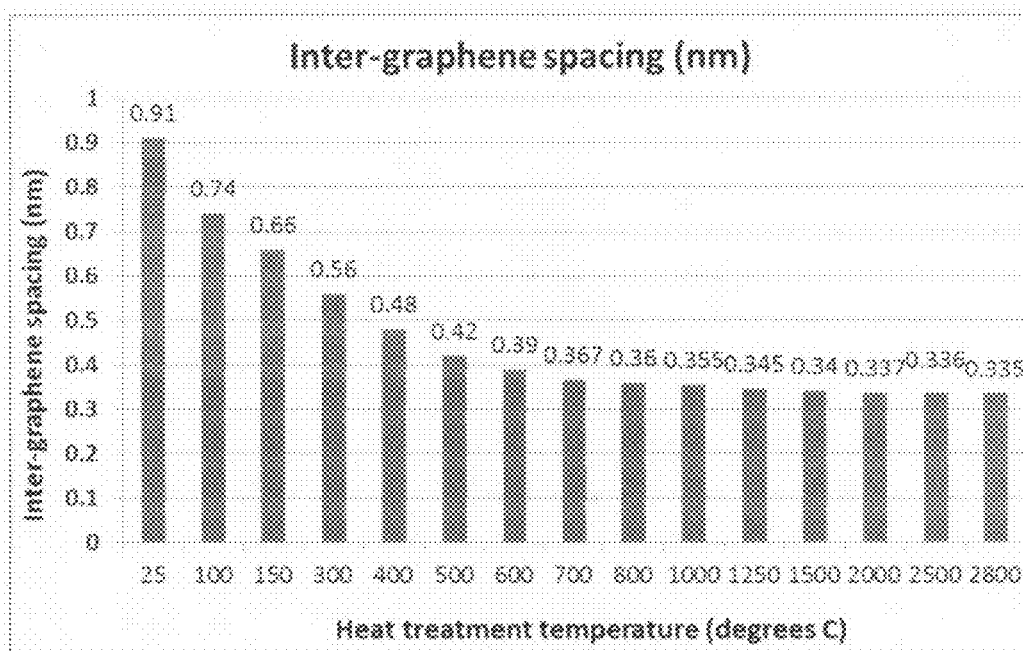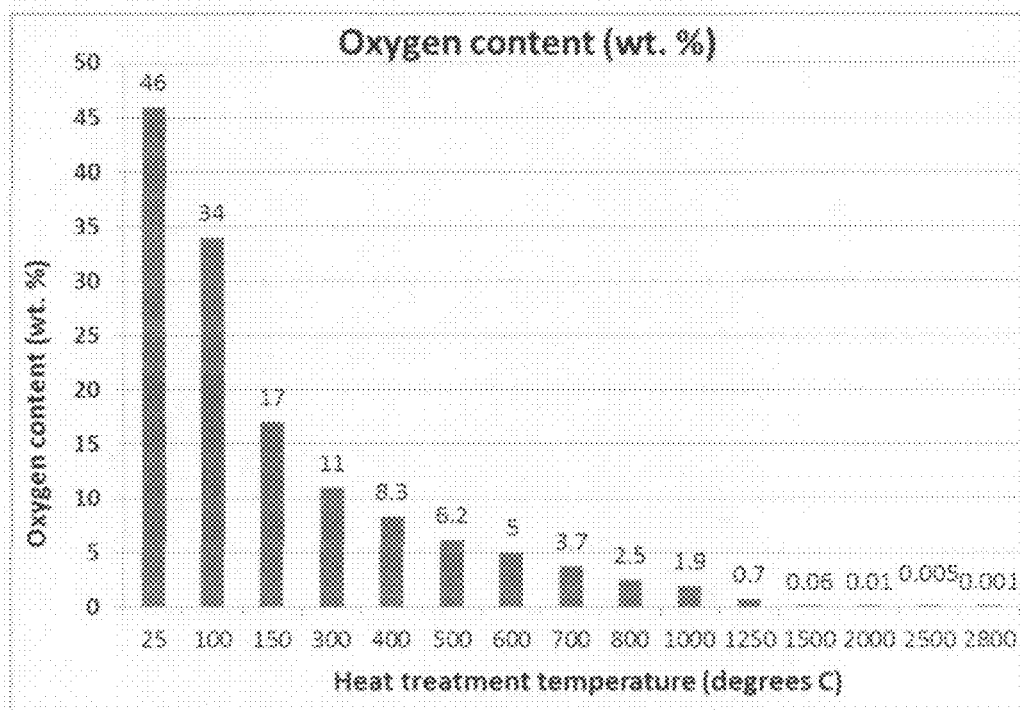**FIG. 4(A)**
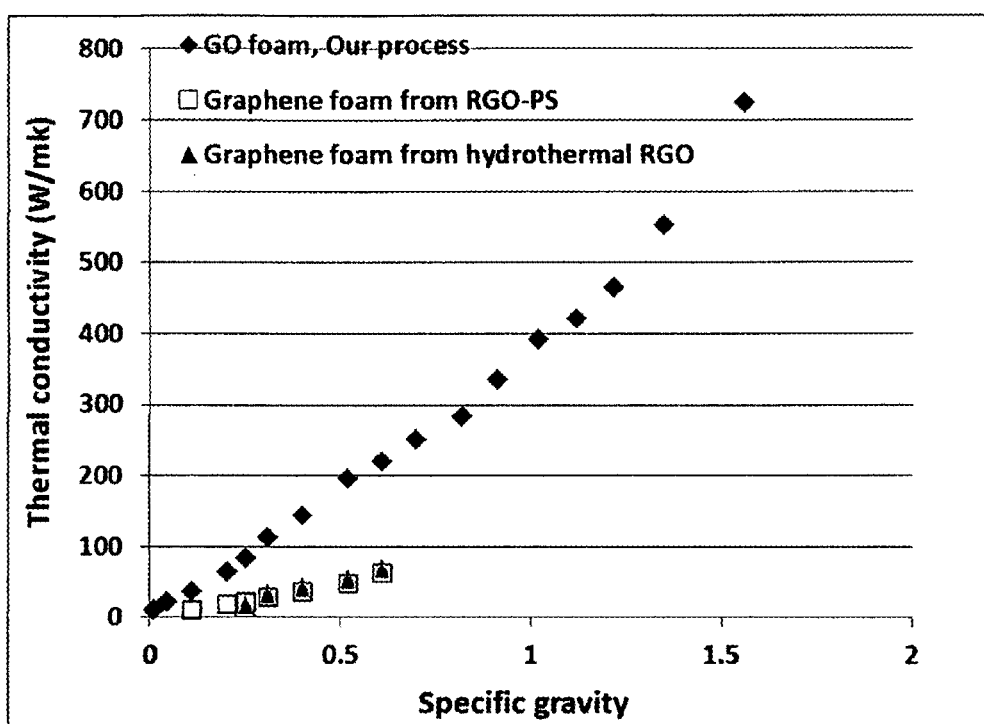
FIG. 4(B)
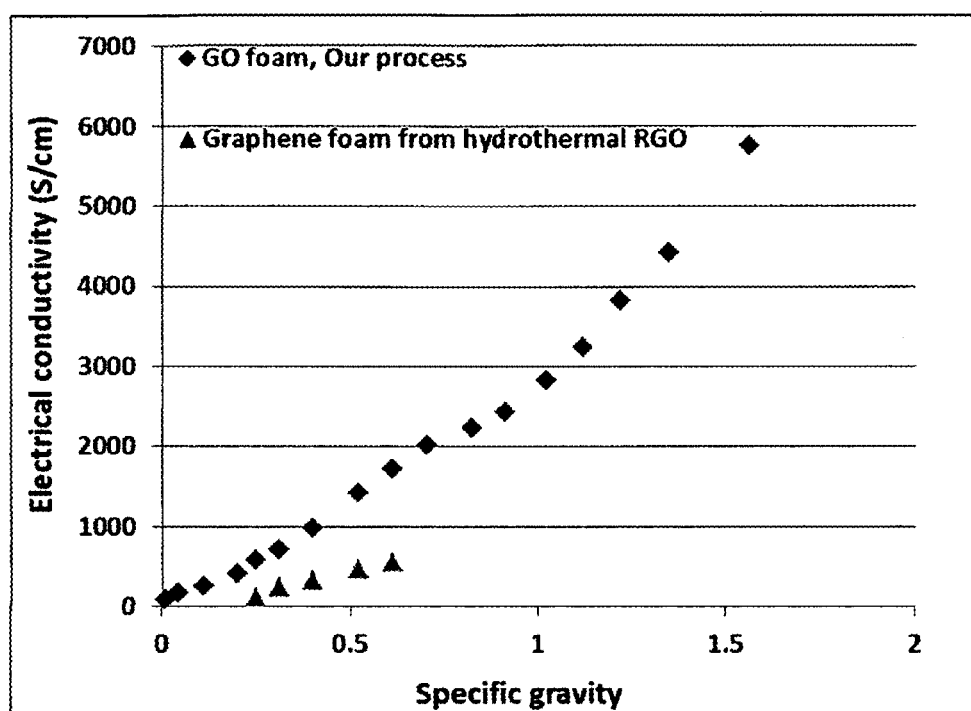
FIG. 4(C)
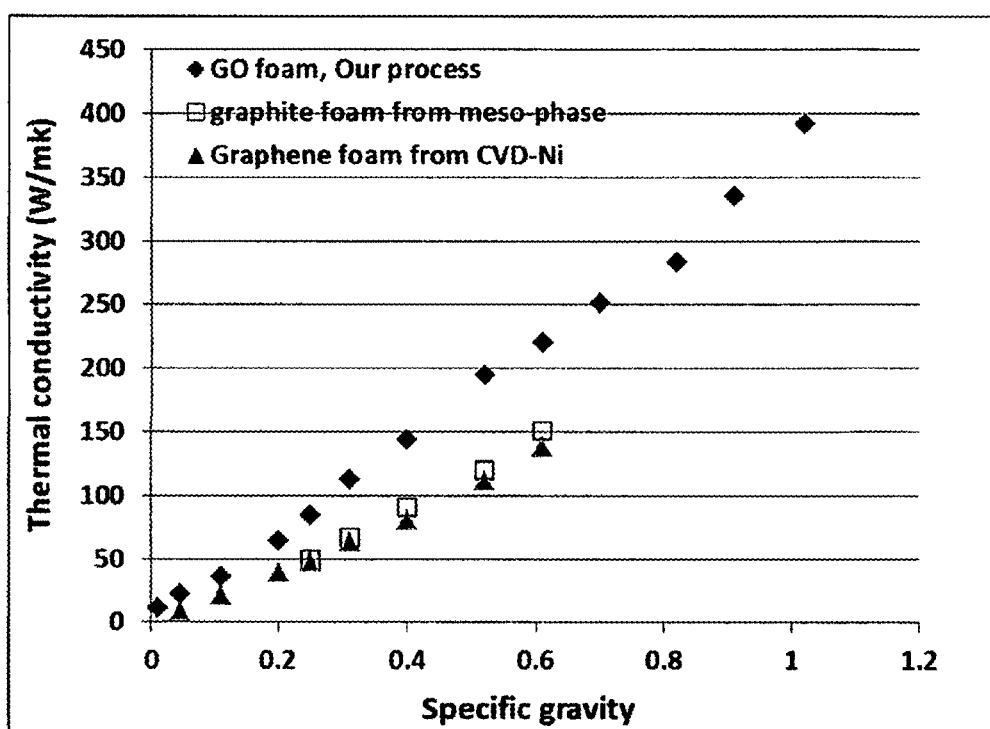
FIG. 5(A)
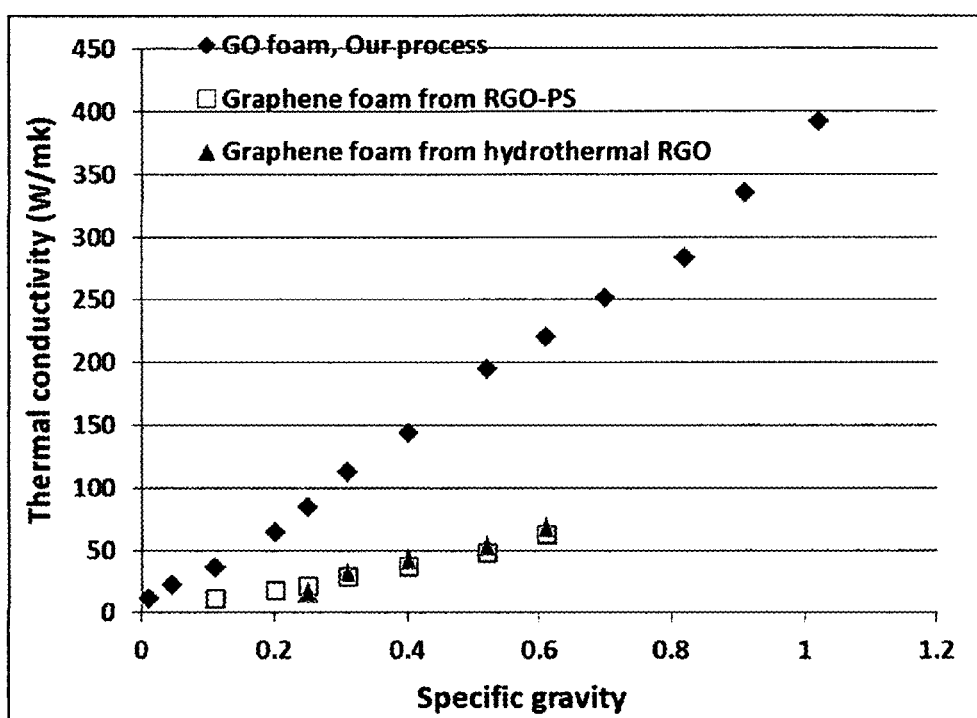
FIG. 5(B)
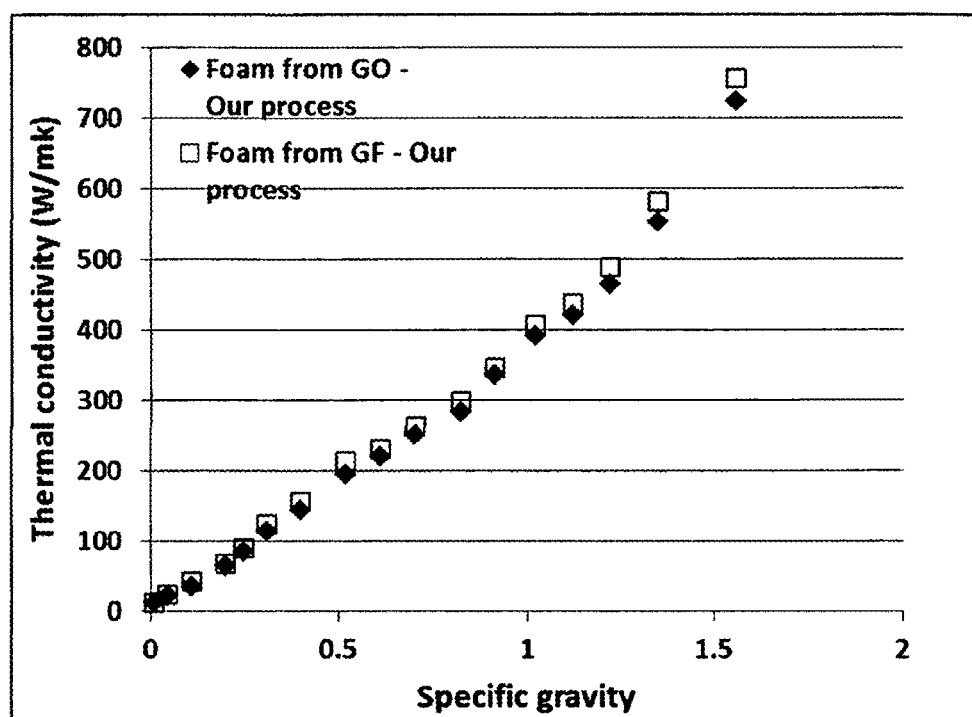
FIG. 6
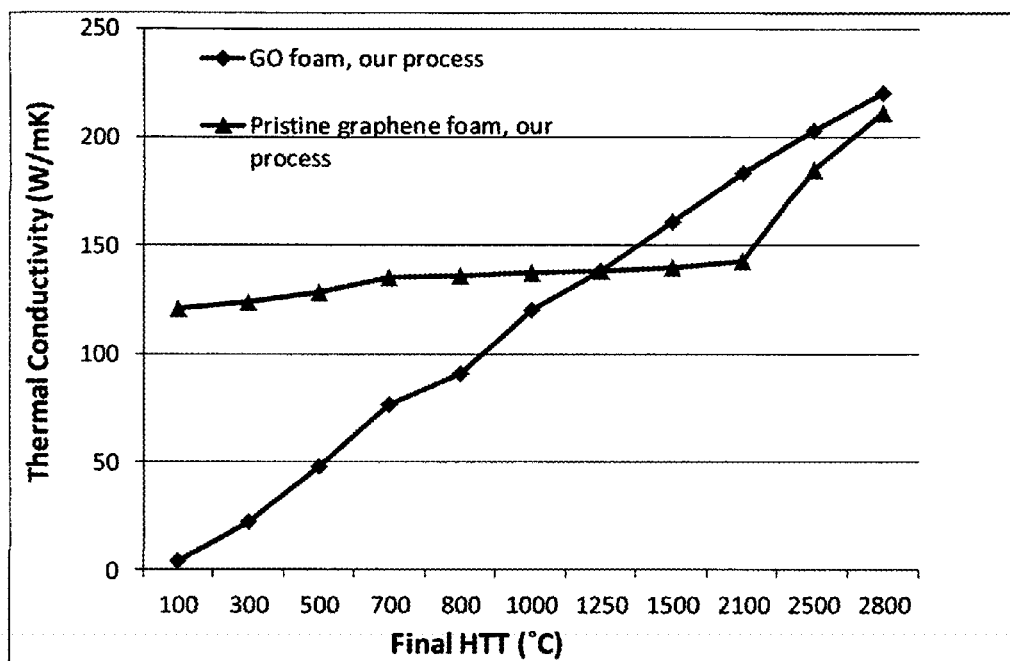
FIG. 7

FIG. 8(A)

FIG. 8(B)
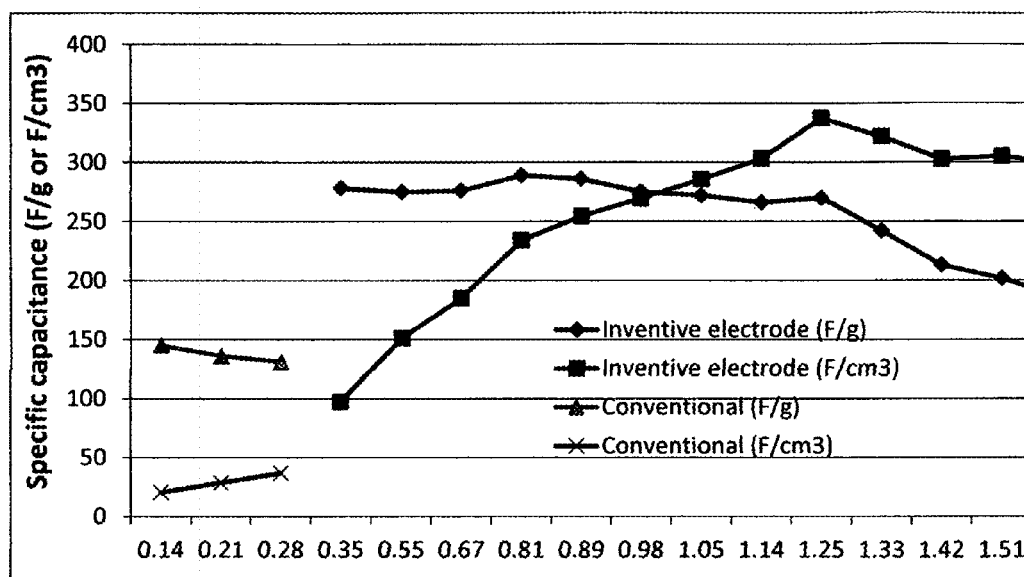
FIG. 9

FIG. 10

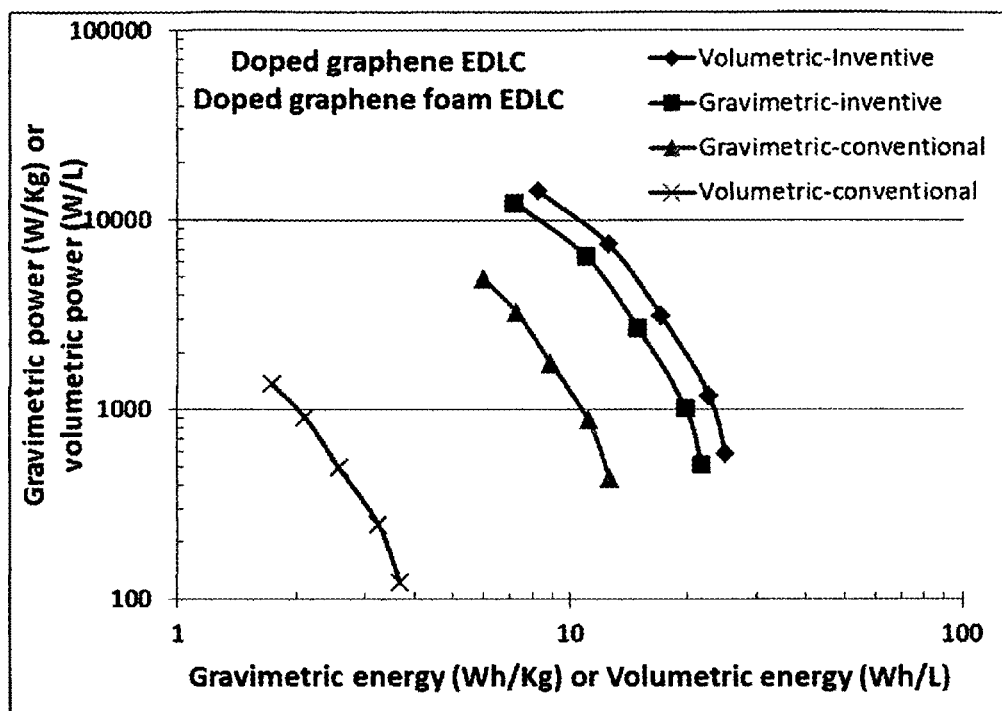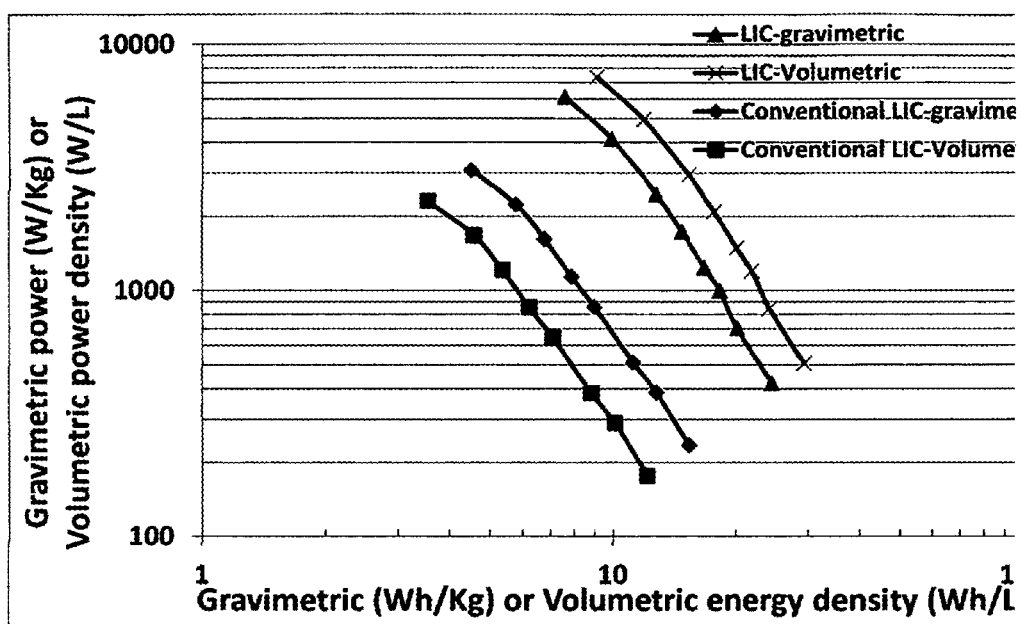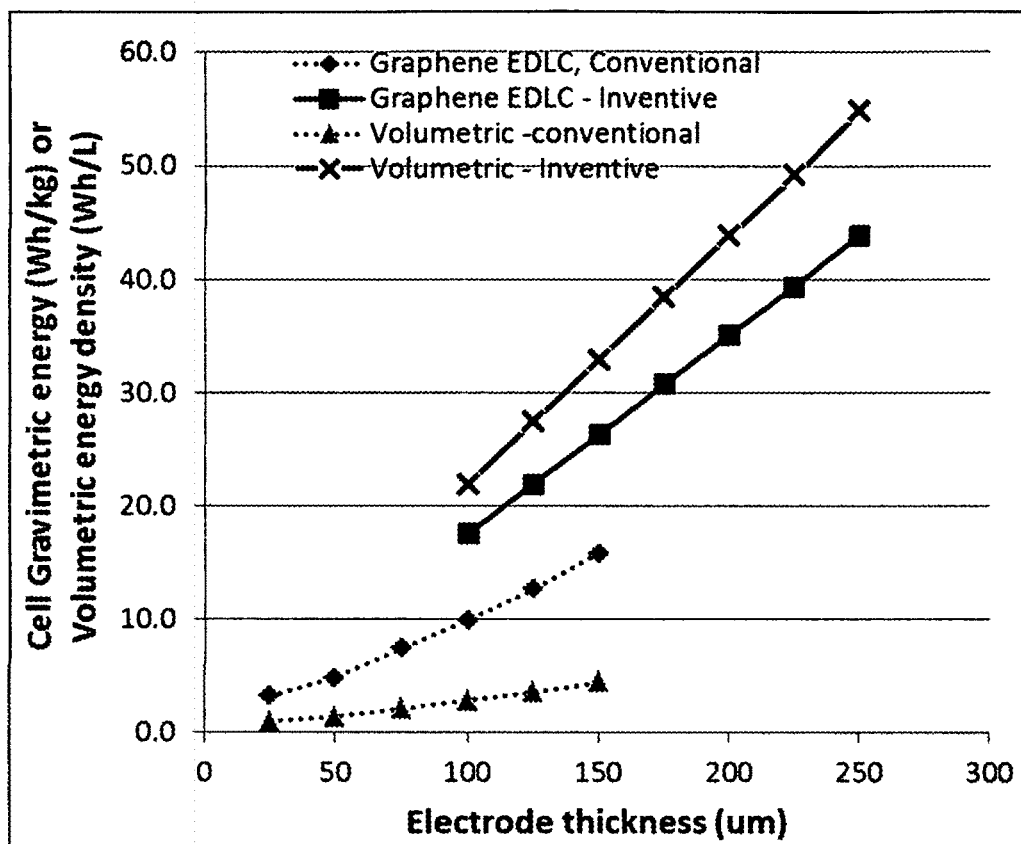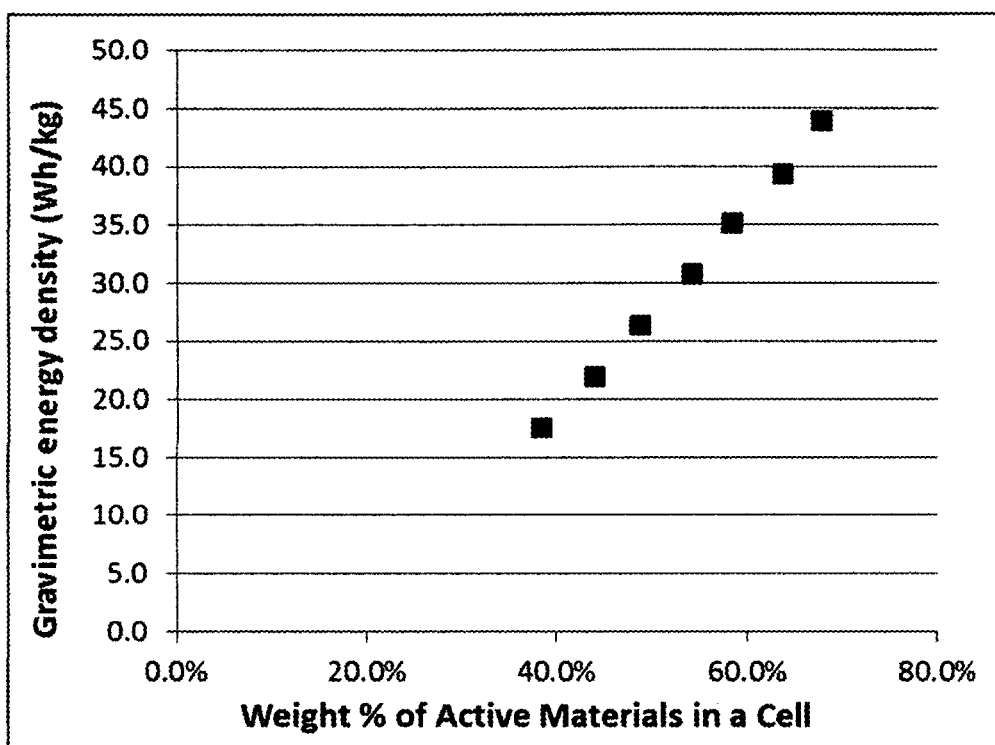FIG. 11

FIG. 12

FIG. 13

PROCESS FOR PRODUCING GRAPHENE FOAM SUPERCAPACITOR ELECTRODE

FIELD OF THE INVENTION

The present invention relates generally to the field of supercapacitor and, more particularly, to a graphene foam-based electrode, a supercapacitor containing such an electrode, and a process for producing same.

BACKGROUND OF THE INVENTION

A Critical Review on Supercapacitors

Electrochemical capacitors (ECs), also known as ultracapacitors or supercapacitors, are being considered for uses in hybrid electric vehicles (EVs) where they can supplement a battery used in an electric car to provide bursts of power needed for rapid acceleration, the biggest technical hurdle to making battery-powered cars commercially viable. A battery would still be used for cruising, but supercapacitors (with their ability to release energy much more quickly than batteries) would kick in whenever the car needs to accelerate for merging, passing, emergency maneuvers, and hill climbing. The EC must also store sufficient energy to provide an acceptable driving range. To be cost-, volume-, and weight-effective compared to additional battery capacity they must combine adequate energy densities (volumetric and gravimetric) and power densities with long cycle life, and meet cost targets as well.

ECs are also gaining acceptance in the electronics industry as system designers become familiar with their attributes and benefits. ECs were originally developed to provide large bursts of driving energy for orbital lasers. In complementary metal oxide semiconductor (CMOS) memory backup applications, for instance, a one-Farad EC having a volume of only one-half cubic inch can replace nickel-cadmium or lithium batteries and provide backup power for months. For a given applied voltage, the stored energy in an EC associated with a given charge is half that storable in a corresponding battery system for passage of the same charge. Nevertheless, ECs are extremely attractive power sources. Compared with batteries, they require no maintenance, offer much higher cycle-life, require a very simple charging circuit, experience no "memory effect," and are generally much safer. Physical rather than chemical energy storage is the key reason for their safe operation and extraordinarily high cycle-life. Perhaps most importantly, capacitors offer higher power density than batteries.

The high volumetric capacitance density of an EC relative to conventional capacitors (10 to 100 times greater than conventional capacitors) derives from using porous electrodes to create a large effective "plate area" and from storing energy in the diffuse double layer. This double layer, created naturally at a solid-electrolyte interface when voltage is imposed, has a thickness of only about 1 nm, thus forming an extremely small effective "plate separation." Such a supercapacitor is commonly referred to as an electric double layer capacitor (EDLC). The double layer capacitor is based on a high surface area electrode material, such as activated carbon, immersed in a liquid electrolyte. A polarized double layer is formed at electrode-electrolyte interfaces providing high capacitance. This implies that the specific capacitance of a supercapacitor is directly proportional to the specific surface area of the electrode material. This surface area must be accessible by electrolyte and the

resulting interfacial zones must be sufficiently large to accommodate the so-called electric double-layer charges.

In some ECs, stored energy is further augmented by pseudo-capacitance effects, occurring again at the solid-electrolyte interface due to electrochemical phenomena such as the redox charge transfer.

However, there are several serious technical issues associated with current state-of-the-art ECs or supercapacitors:

(1) Experience with ECs based on activated carbon electrodes shows that the experimentally measured capacitance is always much lower than the geometrical capacitance calculated from the measured surface area and the width of the dipole layer. For very high surface area activated carbons, typically only about 20 percent of the "theoretical" capacitance was observed. This disappointing performance is related to the presence of micro-pores (<2 nm, mostly <1 nm) and ascribed to inaccessibility of some pores by the electrolyte, wetting deficiencies, and/or the inability of a double layer to form successfully in pores in which the oppositely charged surfaces are less than about 1-2 nm apart. In activated carbons, depending on the source of the carbon and the heat treatment temperature, a surprising amount of surfaces can be in the form of such micro-pores that are not accessible to liquid electrolyte.

(2) Despite the high gravimetric capacitances at the electrode level (based on active material weights alone) as frequently claimed in open literature and patent documents, these electrodes unfortunately fail to provide energy storage devices with high capacities at the supercapacitor cell or pack level (based on the total cell weight or pack weight). This is due to the notion that, in these reports, the actual mass loadings of the electrodes and the apparent densities for the active materials are too low. In most cases, the active material mass loadings of the electrodes (areal density) is significantly lower than 10 mg/cm^2 (areal density=the amount of active materials per electrode cross-sectional area along the electrode thickness direction) and the apparent volume density or tap density of the active material is typically less than 0.75 g/cm^{-3} (more typically less than 0.5 g/cm^{-3} and most typically less than 0.3 g/cm^{-3}) even for relatively large particles of activated carbon.

The low mass loading is primarily due to the inability to obtain thicker electrodes (thicker than 100-200 µm) using the conventional slurry coating procedure. This is not a trivial task as one might think, and in reality the electrode thickness is not a design parameter that can be arbitrarily and freely varied for the purpose of optimizing the cell performance. Contrarily, thicker samples tend to become extremely brittle or of poor structural integrity and would also require the use of large amounts of binder resin. These problems are particularly acute for graphene material-based electrodes. It has not been previously possible to produce graphene-based electrodes that are thicker than 100 µm and remain highly porous with pores remaining fully accessible to liquid electrolyte. The low areal densities and low volume densities (related to thin electrodes and poor packing density) result in relatively low volumetric capacitances and low volumetric energy density of the supercapacitor cells.

With the growing demand for more compact and portable energy storage systems, there is keen interest to increase the utilization of the volume of the energy storage devices. Novel electrode materials and designs that enable high volumetric capacitances and high mass loadings are essential to achieving improved cell volumetric capacitances and energy densities.

(3) During the past decade, much work has been conducted to develop electrode materials with increased volumetric capacitances utilizing porous carbon-based materials, such as graphene, carbon nanotube-based composites, porous graphite oxide, and porous meso carbon. Although these experimental supercapacitors featuring such electrode materials can be charged and discharged at high rates and also exhibit large volumetric electrode capacitances (100 to 200 F/cm^3 in most cases, based on the electrode volume), their typical active mass loading of <1 mg/cm^2, tap density of <0.2 g/cm^{-3}, and electrode thicknesses of up to tens of micrometers (<<100 μm) are still significantly lower than those used in most commercially available electrochemical capacitors (i.e. 10 mg/cm^2, 100-200 μm), which results in energy storage devices with relatively low areal and volumetric capacitances and low volumetric energy densities.

(4) For graphene-based supercapacitors, there are additional problems that remain to be solved, explained below:

Nano graphene materials have recently been found to exhibit exceptionally high thermal conductivity, high electrical conductivity, and high strength. Another outstanding characteristic of graphene is its exceptionally high specific surface area. A single graphene sheet provides a specific external surface area of approximately 2,675 m^2/g (that is accessible by liquid electrolyte), as opposed to the exterior surface area of approximately 1,300 m^2/g provided by a corresponding single-wall CNT (interior surface not accessible by electrolyte). The electrical conductivity of graphene is slightly higher than that of CNTs.

The instant applicants (A. Zhamu and B. Z. Jang) and their colleagues were the first to investigate graphene- and other nano graphite-based nano materials for supercapacitor application [Please see Refs. 1-5 below; the 1st patent application was submitted in 2006 and issued in 2009]. After 2008, researchers began to realize the significance of graphene materials for supercapacitor applications.

LIST OF REFERENCES

1. Lulu Song, A. Zhamu, Jiusheng Guo, and B. Z. Jang "Nano-scaled Graphene Plate Nanocomposites for Supercapacitor Electrodes" U.S. Pat. No. 7,623,340 (Nov. 24, 2009).
2. Aruna Zhamu and Bor Z. Jang, "Process for Producing Nano-scaled Graphene Platelet Nanocomposite Electrodes for Supercapacitors," U.S. patent application Ser. No. 11/906,786 (Oct. 4, 2007).
3. Aruna Zhamu and Bor Z. Jang, "Graphite-Carbon Composite Electrodes for Supercapacitors" U.S. patent application Ser. No. 11/895,657 (Aug. 27, 2007).
4. Aruna Zhamu and Bor Z. Jang, "Method of Producing Graphite-Carbon Composite Electrodes for Supercapacitors" U.S. patent application Ser. No. 11/895,588 (Aug. 27, 2007).
5. Aruna Zhamu and Bor Z. Jang, "Graphene Nanocomposites for Electrochemical cell Electrodes," U.S. patent application Ser. No. 12/220,651 (Jul. 28, 2008).

However, individual nano graphene sheets have a great tendency to re-stack themselves, effectively reducing the specific surface areas that are accessible by the electrolyte in a supercapacitor electrode. The significance of this graphene sheet overlap issue may be illustrated as follows: For a nano graphene platelet with dimensions of l (length)×w (width)×t (thickness) and density ρ, the estimated surface area per unit mass is $S/m=(2/\rho)(1/l+1/w+1/t)$. With $\rho=2.2$ g/cm^3, l=100 nm, w=100 nm, and t=0.34 nm (single layer), we have an impressive S/m value of 2,675 m^2/g, which is much greater than that of most commercially available carbon black or activated carbon materials used in the state-of-the-art supercapacitor. If two single-layer graphene sheets stack to form a double-layer graphene, the specific surface area is reduced to 1,345 m^2/g. For a three-layer graphene, t=1 nm, we have $S/m=906$ m^2/g. If more layers are stacked together, the specific surface area would be further significantly reduced.

These calculations suggest that it is critically important to find a way to prevent individual graphene sheets from re-stacking and, even if they partially re-stack, the resulting multi-layer structure would still have inter-layer pores of adequate sizes. These pores must be sufficiently large to allow for accessibility by the electrolyte and to enable the formation of electric double-layer charges, which presumably require a pore size of at least 1-2 nm. However, these pores or inter-graphene spacings must also be sufficiently small to ensure a large tap density. Unfortunately, the typical tap density of graphene-based electrode produced by the conventional process is less than 0.3 g/cm^3, and most typically <<0.2 g/cm^3. To a great extent, the requirement to have large pore sizes and high porosity level and the requirement to have a high tap density are considered mutually exclusive in supercapacitors.

Another major technical barrier to using graphene sheets as a supercapacitor electrode active material is the challenge of forming a thick active material layer onto the surface of a solid current collector (e.g. Al foil) using the conventional graphene-solvent slurry coating process. In such an electrode, the graphene electrode typically requires a large amount of a binder resin (hence, significantly reduced active material proportion vs. non-active or overhead materials/ components). In addition, any electrode prepared in this manner that is thicker than 50 μm is brittle and weak. There has been no effective solution to these problems.

Therefore, there is clear and urgent need for supercapacitors that have high active material mass loading (high areal density), active materials with high apparent density (high tap density), high electrode thickness without significantly decreasing the electron and ion transport rates (e.g. without a long electron transport distance), high volumetric capacitance, and high volumetric energy density. For graphene-based electrodes, one must also overcome problems such as re-stacking of graphene sheets, the demand for large proportion of a binder resin, and difficulty in producing thick graphene electrode layers.

Carbon is known to have five unique crystalline structures, including diamond, fullerene (0-D nano graphitic material), carbon nano-tube or carbon nano-fiber (1-D nano graphitic material), graphene (2-D nano graphitic material), and graphite (3-D graphitic material). The carbon nano-tube (CNT) refers to a tubular structure grown with a single wall or multi-wall. Carbon nano-tubes (CNTs) and carbon nano-fibers (CNFs) have a diameter on the order of a few nanometers to a few hundred nanometers. Their longitudinal, hollow structures impart unique mechanical, electrical and chemical properties to the material. The CNT or CNF is a one-dimensional nano carbon or 1-D nano graphite material.

Our research group was among the first to discover graphene [B. Z. Jang and W. C. Huang, "Nano-scaled Graphene Plates," U.S. patent application Ser. No. 10/274, 473, submitted on Oct. 21, 2002; now U.S. Pat. No. 7,071, 258 (Jul. 4, 2006)]. The processes for producing NGPs and NGP nanocomposites were recently reviewed by us [Bor Z.

Jang and A Zhamu, "Processing of Nano Graphene Platelets (NGPs) and NGP Nanocomposites: A Review," J. Materials Sci. 43 (2008) 5092-5101].

For the purpose of defining the claims of the instant application, NGPs or graphene materials include discrete sheets/platelets of single-layer and multi-layer (typically less than 10 layers) pristine graphene, graphene oxide, reduced graphene oxide (RGO), graphene fluoride, graphene chloride, graphene bromide, graphene iodide, hydrogenated graphene, nitrogenated graphene, chemically functionalized graphene, doped graphene (e.g. doped by B or N). Pristine graphene has essentially 0% oxygen. RGO typically has an oxygen content of 0.001%-5% by weight. Graphene oxide (including RGO) can have 0.001%-50% by weight of oxygen. Other than pristine graphene, all the graphene materials have 0.001%-50% by weight of non-carbon elements (e.g. O, H, N, B, F, Cl, Br, I, etc.). These materials are herein referred to as non-pristine graphene materials. The presently invented graphene-carbon foam can contain pristine or non-pristine graphene and the invented method allows for this flexibility.

A Review on Production of Graphene Foams

Generally speaking, a foam or foamed material is composed of pores (or cells) and pore walls (a solid material). The pores can be interconnected to form an open-cell foam. A graphene foam is composed of pores and pore walls that contain a graphene material. There are three major methods of producing graphene foams:

The first method is the hydrothermal reduction of graphene oxide hydrogel that typically involves sealing graphene oxide (GO) aqueous suspension in a high-pressure autoclave and heating the GO suspension under a high pressure (tens or hundreds of atm) at a temperature typically in the range of 180-300° C. for an extended period of time (typically 12-36 hours). A useful reference for this method is given here: Y. Xu, et al. "Self-Assembled Graphene Hydrogel via a One-Step Hydrothermal Process," ACS Nano 2010, 4, 4324-4330. There are several major issues associated with this method: (a) The high pressure requirement makes it an impractical method for industrial-scale production. For one thing, this process cannot be conducted on a continuous basis. (b) It is difficult, if not impossible, to exercise control over the pore size and the porosity level of the resulting porous structure. (c) There is no flexibility in terms of varying the shape and size of the resulting reduced graphene oxide (RGO) material (e.g. it cannot be made into a film shape). (d) The method involves the use of an ultra-low concentration of GO suspended in water (e.g. 2 mg/mL=2 g/L=2 kg/kL). With the removal of non-carbon elements (up to 50%), one can only produce less than 2 kg of graphene material (RGO) per 1000-liter suspension. Furthermore, it is practically impossible to operate a 1000-liter reactor that has to withstand the conditions of a high temperature and a high pressure. Clearly, this is not a scalable process for mass production of porous graphene structures.

The second method is based on a template-assisted catalytic CVD process, which involves CVD deposition of graphene on a sacrificial template (e.g. Ni foam). The graphene material conforms to the shape and dimensions of the Ni' foam structure. The Ni foam is then etched away using an etching agent, leaving behind a monolith of graphene skeleton that is essentially an open-cell foam. A useful reference for this method is given here: Zongping Chen, et al., "Three-dimensional flexible and conductive intercon-

nected graphene networks grown by chemical vapour deposition," Nature Materials, 10 (June 2011) 424-428. There are several problems associated with such a process: (a) the catalytic CVD is intrinsically a very slow, highly energy-intensive, and expensive process; (b) the etching agent is typically a highly undesirable chemical and the resulting Ni-containing etching solution is a source of pollution. It is very difficult and expensive to recover or recycle the dissolved Ni metal from the etchant solution. (c) It is challenging to maintain the shape and dimensions of the graphene foam without damaging the cell walls when the Ni foam is being etched away. The resulting graphene foam is typically very brittle and fragile. (d) The transport of the CVD precursor gas (e.g. hydrocarbon) into the interior of a metal foam can be difficult, resulting in a non-uniform structure, since certain spots inside the sacrificial metal foam may not be accessible to the CVD precursor gas.

The third method of producing graphene foam also makes use of a sacrificial material (e.g. colloidal polystyrene particles, PS) that is coated with graphene oxide sheets using a self-assembly approach. For instance, Choi, et al. prepared chemically modified graphene (CMG) paper in two steps: fabrication of free-standing PS/CMG films by vacuum filtration of a mixed aqueous colloidal suspension of CMG and PS (2.0 μm PS spheres), followed by removal of PS beads to generate 3D macro-pores. [B. G. Choi, et al., "3D Macroporous Graphene Frameworks for Supercapacitors with High Energy and Power Densities," ACS Nano, 6 (2012) 4020-4028.] Choi, et al. fabricated well-ordered free-standing PS/CMG paper by filtration, which began with separately preparing a negatively charged CMG colloidal and a positively charged PS suspension. A mixture of CMG colloidal and PS suspension was dispersed in solution under controlled pH (=2), where the two compounds had the same surface charges (zeta potential values of +13±2.4 mV for CMG and +68±5.6 mV for PS). When the pH was raised to 6, CMGs (zeta potential=−29±3.7 mV) and PS spheres (zeta potential=+51±2.5 mV) were assembled due to the electrostatic interactions and hydrophobic characteristics between them, and these were subsequently integrated into PS/CMG composite paper through a filtering process. This method also has several shortcomings: (a) This method requires very tedious chemical treatments of both graphene oxide and PS particles. (b) The removal of PS by toluene also leads to weakened macro-porous structures. (c) Toluene is a highly regulated chemical and must be treated with extreme caution. (d) The pore sizes are typically excessively big (e.g. several μm), too big for many useful applications.

The above discussion clearly indicates that every prior art method or process for producing graphene foams has major deficiencies. Thus, it is an object of the present invention to provide a cost-effective process for producing highly conductive, mechanically robust graphene-based foams (specifically, integral 3D graphene foam as a supercapacitor electrode) in large quantities. This process enables the flexible design and control of the porosity level and pore sizes.

It is another object of the present invention to provide a process for producing graphene foam-based supercapacitor electrode that exhibit a thermal conductivity, electrical conductivity, elastic modulus, and/or strength that are comparable to or greater than those of the conventional graphite or carbon foam-based electrode.

Yet another object of the present invention is to provide a supercapacitor electrode based on (a) a pristine graphene foam that contains essentially all carbon only and preferably have a pore size range of 0.5-50 nm); and (b) non-pristine

graphene foams (graphene fluoride, graphene chloride, nitrogenated graphene, etc.) that contains at least 0.001% by weight (typically from 0.01% to 25% by weight and most typically from 0.1% to 20%) of non-carbon elements.

Another object of the present invention is to provide a supercapacitor that contains a graphene foam-based electrode of the present invention.

SUMMARY OF THE INVENTION

The present invention provides a supercapacitor electrode containing a solid graphene foam as an electrode active material. The graphene foam is pre-impregnated with a liquid or gel electrolyte. The liquid electrolyte may contain an aqueous electrolyte, organic electrolyte, ionic liquid electrolyte, or a mixture of an organic and an ionic liquid electrolyte.

The solid graphene foam is composed of multiple pores and pore walls, wherein the pore walls contain a pristine graphene material having essentially zero % of non-carbon elements, or a non-pristine graphene material having from 0.001% to 5% by weight of non-carbon elements wherein the non-pristine graphene is selected from graphene oxide, reduced graphene oxide, graphene fluoride, graphene chloride, graphene bromide, graphene iodide, hydrogenated graphene, nitrogenated graphene, chemically functionalized graphene, doped graphene, or a combination thereof, and the solid graphene foam has a density from 0.01 to 1.7 g/cm^3, a specific surface area from 50 to 3,300 m^2/g, a thermal conductivity of at least 200 W/mK per unit of specific gravity, and/or an electrical conductivity no less than 2,000 S/cm per unit of specific gravity. In a preferred embodiment, the pore walls contain stacked graphene planes having an inter-plane spacing d_{002} from 0.3354 nm to 0.36 nm as measured by X-ray diffraction.

In an embodiment, the pore walls contain a pristine graphene and the solid graphene foam has a density from 0.1 to 1.7 g/cm^3 or an average pore size from 0.5 nm to 50 nm. In an embodiment, the pore walls contain a non-pristine graphene material selected from the group consisting of graphene oxide, reduced graphene oxide, graphene fluoride, graphene chloride, graphene bromide, graphene iodide, hydrogenated graphene, nitrogenated graphene, chemically functionalized graphene, and combinations thereof, and wherein the solid graphene foam contains a content of non-carbon elements in the range of 0.01% to 2.0% by weight. In other words, the non-carbon elements can include an element selected from oxygen, fluorine, chlorine, bromine, iodine, nitrogen, hydrogen, or boron. In a specific embodiment, the pore walls contain graphene fluoride and the solid graphene foam contains a fluorine content from 0.01% to 2.0% by weight. In another embodiment, the pore walls contain graphene oxide and said solid graphene foam contains an oxygen content from 0.01% to 2.0% by weight. In an embodiment, the solid graphene foam has a specific surface area from 200 to 2,800 m^2/g or a density from 0.1 to 1.5 g/cm^3. The non-carbon elements include an element selected from oxygen, fluorine, chlorine, bromine, iodine, nitrogen, hydrogen, or boron.

In a preferred embodiment, the solid graphene foam is made into a continuous-length roll sheet form (a roll of a continuous foam sheet) having a thickness from 10 nm to 10 mm and a length of at least 1 meter long, preferably at least 2 meters, further preferably at least 10 meters, and most preferably at least 100 meters. This sheet roll is produced by a roll-to-roll process. There has been no prior art graphene foam that is made into a sheet roll form. It has not been

previously found or suggested possible to have a roll-to-roll process for producing a continuous length of graphene foam, either pristine or non-pristine.

In certain desired embodiments, the solid graphene foam further contains a carbon or graphite material selected from carbon nanotubes, carbon nano-fibers, carbon fiber segments, graphite fiber segments, activated carbon, carbon black particles, carbon wires, natural graphite particles, needle coke particles, meso-carbon micro-beads, particles of a natural or artificial graphite, expanded graphite flakes, or a combination thereof. These carbon or graphite materials can be easily incorporated into the graphene suspension prior to a coating procedure.

In order to increase the specific capacitance and specific energy of the supercapacitor, the multiple pores may contain a redox pair partner selected from an intrinsically conductive polymer, a transition metal oxide, and/or an organic molecule, wherein said redox pair partner is in physical or electronic contact with said graphene material, forming a redox pair therewith. The intrinsically conducting polymer may be selected from polyaniline, polypyrrole, polythiophene, polyfuran, sulfonated polyaniline, sulfonated polypyrrole, sulfonated polythiophene, sulfonated polyfuran, sulfonated polyacetylene, or a combination thereof.

In a preferred embodiment, the graphene foam has an oxygen content or non-carbon content less than 1% by weight, and the pore walls have stacked graphene planes having an inter-graphene spacing less than 0.35 nm, a thermal conductivity of at least 250 W/mK per unit of specific gravity, and/or an electrical conductivity no less than 2,500 S/cm per unit of specific gravity. In a further preferred embodiment, the graphene foam has an oxygen content or non-carbon content less than 0.01% by weight and said pore walls contain stacked graphene planes having an inter-graphene spacing less than 0.34 nm, a thermal conductivity of at least 300 W/mK per unit of specific gravity, and/or an electrical conductivity no less than 3,000 S/cm per unit of specific gravity.

In yet another preferred embodiment, the graphene foam has an oxygen content or non-carbon content no greater than 0.01% by weight and said pore walls contain stacked graphene planes having an inter-graphene spacing less than 0.336 nm, a mosaic spread value no greater than 0.7, a thermal conductivity of at least 350 W/mK per unit of specific gravity, and/or an electrical conductivity no less than 3,500 S/cm per unit of specific gravity. In still another preferred embodiment, the graphene foam has pore walls containing stacked graphene planes having an inter-graphene spacing less than 0.336 nm, a mosaic spread value no greater than 0.4, a thermal conductivity greater than 400 W/mK per unit of specific gravity, and/or an electrical conductivity greater than 4,000 S/cm per unit of specific gravity.

In a preferred embodiment, the pore walls contain stacked graphene planes having an inter-graphene spacing less than 0.337 nm and a mosaic spread value less than 1.0. In a preferred embodiment, the graphene foam exhibits a degree of graphitization no less than 80% (preferably no less than 90%) and/or a mosaic spread value less than 0.4. In a preferred embodiment, the pore walls contain a 3D network of interconnected graphene planes.

In a preferred embodiment, the solid graphene foam contains pores having an average pore size from 0.5 nm to 50 nm. The solid graphene foam can also be made to contain micron-scaled pores (1-500 μm).

The present invention also provides a supercapacitor comprising an anode, a porous separator-electrolyte layer or

electrolyte-permeable membrane, and a cathode, wherein either or both of the anode and the cathode contains the presently invented electrode. If both the anode and the cathode contain such an electrode and the two electrodes have identical compositions, we have a symmetric supercapacitor. If the electrode contains only a graphene material or a graphene and a carbon or graphite material as the only electrode active material, we have an electric double layer capacitor (EDLC). The presently invented supercapacitor electrode is capable of delivering a specific capacitance of 150-350 F/g (based on the electric double layer capacitance alone), in contrast to the typical EDLC-based specific capacitance of 100-170 F/g of prior art graphene-based EDLC supercapacitors.

If at least an electrode contains a redox pair (e.g. graphene and an intrinsically conductive polymer or transition metal oxide), we have a redox or pseudo-capacitor. The supercapacitor is a lithium-ion capacitor or sodium-ion capacitor if the cathode contains the presently invented electrode (having graphene or graphene-carbon material mixture as the electrode active material) and the anode contains a pre-lithiated anode active material (e.g. pre-lithiated graphite or Si particles) or a pre-sodiated anode active material (e.g. pre-sodiated hard carbon particles).

The presently invented solid graphene foam may be produced by a process comprising:

(a) preparing a graphene dispersion having a graphene material dispersed in a liquid medium, wherein the graphene material is selected from pristine graphene, graphene oxide, reduced graphene oxide, graphene fluoride, graphene chloride, graphene bromide, graphene iodide, hydrogenated graphene, nitrogenated graphene, chemically functionalized graphene, doped graphene, or a combination thereof and wherein the dispersion contains an optional blowing agent;

(b) dispensing and depositing the graphene dispersion onto a surface of a supporting substrate (e.g. plastic film, rubber sheet, metal foil, glass sheet, paper sheet, etc.) to form a wet layer of graphene material, wherein the dispensing and depositing procedure includes subjecting the graphene dispersion to an orientation-inducing stress;

(c) partially or completely removing the liquid medium from the wet layer of graphene material to form a dried layer of graphene material having a content of non-carbon elements (e.g. O, H, N, B, F, Cl, Br, I, etc.) no less than 5% by weight;

(d) heat treating the dried layer of graphene material at a first heat treatment temperature from 100° C. to 3,200° C. at a desired heating rate sufficient to induce volatile gas molecules from the non-carbon elements or to activate said blowing agent for producing the solid graphene foam having a density from 0.01 to 1.7 g/cm³ (more typically from 0.1 to 1.7 g/cm³, and even more typically from 0.3 to 1.5 g/cm³, and most typically from 0.5 to 0.1.3 g/cm³), or a specific surface area from 50 to 3,200 m²/g (more typically from 200 to 2,800 m²/g, and most typically from 500 to 2,500 m²/g); and

(e) impregnating said multiple pores with a liquid electrolyte or gel electrolyte to form a layer of pre-impregnated solid graphene foam, which is subjected to a step of compressing or roll-pressing that reduces a pore size, improve orientation of graphene planes, and squeeze excess electrolyte out of the pre-impregnated solid graphene foam for forming the supercapacitor electrode.

The process may further include a step of heat-treating the solid graphene foam at a second heat treatment temperature higher than the first heat treatment temperature, prior to step (e), for a length of time sufficient for obtaining a graphene foam wherein the pore walls contain stacked graphene

planes having an inter-plane spacing d_{002} from 0.3354 nm to 0.36 nm and a content of non-carbon elements less than 2% by weight.

This optional blowing agent is not required if the graphene material has a content of non-carbon elements (e.g. O, H, N, B, F, Cl, Br, I, etc.) no less than 5% by weight (preferably no less than 10%, further preferably no less than 20%, even more preferably no less than 30% or 40%, and most preferably up to 50%). The subsequent high temperature treatment serves to remove a majority of these non-carbon elements from the graphene material, generating volatile gas species that produce pores or cells in the solid graphene material structure. In other words, quite surprisingly, these non-carbon elements play the role of a blowing agent. Hence, an externally added blowing agent is optional (not required). However, the use of a blowing agent can provide added flexibility in regulating or adjusting the porosity level and pore sizes for a desired application. The blowing agent is typically required if the non-carbon element content is less than 5%, such as pristine graphene that is essentially all-carbon.

The blowing agent can be a physical blowing agent, a chemical blowing agent, a mixture thereof, a dissolution-and-leaching agent, or a mechanically introduced blowing agent.

The process may further include a step of heat-treating the solid graphene foam at a second heat treatment temperature higher than the first heat treatment temperature for a length of time sufficient for obtaining a graphene foam wherein the pore walls contain stacked graphene planes having an inter-plane spacing d_{002} from 0.3354 nm to 0.40 nm and a content of non-carbon elements less than 5% by weight (typically from 0.001% to 2%). When the resulting non-carbon element content is from 0.1% to 2.0%, the inter-plane spacing d_{002} is typically from 0.337 nm to 0.40 nm.

If the original graphene material in the dispersion contains a non-carbon element content higher than 5% by weight, the graphene material in the solid graphene foam (after the heat treatment) contains structural defects that are induced during the step (d) of heat treating. The liquid medium can be simply water and/or an alcohol, which is environmentally benign.

In a preferred embodiment, the process is a roll-to-roll process wherein steps (b) and (c) include feeding the supporting substrate from a feeder roller to a deposition zone, continuously or intermittently depositing the graphene dispersion onto a surface of the supporting substrate to form the wet layer of graphene material thereon, drying the wet layer of graphene material to form the dried layer of graphene material, and collecting the dried layer of graphene material deposited on the supporting substrate on a collector roller. Such a roll-to-roll or reel-to-reel process is a truly industrial-scale, massive manufacturing process that can be automated.

In one embodiment, the first heat treatment temperature is from 100° C. to 1,500° C. In another embodiment, the second heat treatment temperature includes at least a temperature selected from (A) 300-1,500° C., (B) 1,500-2,500° C., and/or (C) 2,500-3,200° C. In a specific embodiment, the second heat treatment temperature includes a temperature in the range of 300-1,500° C. for at least 1 hour and then a temperature in the range of 1,500-3,200° C. for at least 1 hour.

There are several surprising results of conducting first and/or second heat treatments to the dried graphene layer, and different heat treatment temperature ranges enable us to achieve different purposes, such as (a) removal of non-carbon elements from the graphene material (e.g. thermal

reduction of fluorinated graphene to obtain graphene or reduced graphene fluoride, RGF)) which generate volatile gases to produce pores or cells in a graphene material, (b) activation of the chemical or physical blowing agent to produce pores or cells, (c) chemical merging or linking of graphene sheets to significantly increase the lateral dimension of graphene sheets in the foam walls (solid portion of the foam), (d) healing of defects created during fluorination, oxidation, or nitrogenation of graphene planes in a graphite particle, and (e) re-organization and perfection of graphitic domains or graphite crystals. These different purposes or functions are achieved to different extents within different temperature ranges. The non-carbon elements typically include an element selected from oxygen, fluorine, chlorine, bromine, iodine, nitrogen, hydrogen, or boron. Quite surprisingly, even under low-temperature foaming conditions, heat-treating induces chemical linking, merging, or chemical bonding between graphene sheets, often in an edge-to-edge manner (some in face-to-face manner).

In one embodiment, the sheet of solid graphene foam has a specific surface area from 200 to 2,500 m^2/g. In one embodiment, the sheet of solid graphene foam has a density from 0.1 to 1.5 g/cm^3. In an embodiment, step (d) of heat treating the layer of graphene material at a first heat treatment temperature is conducted under a compressive stress. In another embodiment, the process comprises a compression step to reduce a thickness, pore size, or porosity level of the sheet of graphene foam. In some applications, the graphene foam has a thickness no greater than 200 μm.

In an embodiment, the graphene dispersion has at least 3% by weight of graphene oxide dispersed in the liquid medium to form a liquid crystal phase. In another embodiment, the graphene dispersion contains a graphene oxide dispersion prepared by immersing a graphitic material in a powder or fibrous form in an oxidizing liquid in a reaction vessel at a reaction temperature for a length of time sufficient to obtain the graphene dispersion wherein the graphitic material is selected from natural graphite, artificial graphite, meso-phase carbon, meso-phase pitch, meso-carbon micro-bead, soft carbon, hard carbon, coke, carbon fiber, carbon nano-fiber, carbon nano-tube, or a combination thereof and wherein the graphene oxide has an oxygen content no less than 5% by weight.

In an embodiment, the first heat treatment temperature contains a temperature in the range of 80° C.-300° C. and, as a result, the graphene foam has an oxygen content or non-carbon element content less than 5%, and the pore walls have an inter-graphene spacing less than 0.40 nm, a thermal conductivity of at least 150 W/mK (more typically at least 200 W/mk) per unit of specific gravity, and/or an electrical conductivity no less than 2,000 S/cm per unit of specific gravity.

In a preferred embodiment, the first and/or second heat treatment temperature contains a temperature in the range of 300° C.-1,500° C. and, as a result, the graphene foam has an oxygen content or non-carbon content less than 1%, and the pore walls have an inter-graphene spacing less than 0.35 nm, a thermal conductivity of at least 250 W/mK per unit of specific gravity, and/or an electrical conductivity no less than 2,500 S/cm per unit of specific gravity. When the first and/or second heat treatment temperature contains a temperature in the range of 1,500° C.-2,100° C., the graphene foam has an oxygen content or non-carbon content less than 0.01% and pore walls have an inter-graphene spacing less than 0.34 nm, a thermal conductivity of at least 300 W/mK per unit of specific gravity, and/or an electrical conductivity no less than 3,000 S/cm per unit of specific gravity.

When the first and/or second heat treatment temperature contains a temperature greater than 2,100° C., the graphene foam has an oxygen content or non-carbon content no greater than 0.001% and pore walls have an inter-graphene spacing less than 0.336 nm, a mosaic spread value no greater than 0.7, a thermal conductivity of at least 350 W/mK per unit of specific gravity, and/or an electrical conductivity no less than 3,500 S/cm per unit of specific gravity. If the first and/or second heat treatment temperature contains a temperature no less than 2,500° C., the graphene foam has pore walls containing stacked graphene planes having an inter-graphene spacing less than 0.336 nm, a mosaic spread value no greater than 0.4, and a thermal conductivity greater than 400 W/mK per unit of specific gravity, and/or an electrical conductivity greater than 4,000 S/cm per unit of specific gravity.

In one embodiment, the pore walls contain stacked graphene planes having an inter-graphene spacing less than 0.337 nm and a mosaic spread value less than 1.0. In another embodiment, the solid wall portion of the graphene foam exhibits a degree of graphitization no less than 80% and/or a mosaic spread value less than 0.4. In yet another embodiment, the solid wall portion of the graphene foam exhibits a degree of graphitization no less than 90% and/or a mosaic spread value no greater than 0.4.

Typically, the pore walls contain a 3D network of inter-connected graphene planes that are electron-conducting pathways. The cell walls contain graphitic domains or graphite crystals having a lateral dimension (L_a, length or width) no less than 20 nm, more typically and preferably no less than 40 nm, still more typically and preferably no less than 100 nm, still more typically and preferably no less than 500 nm, often greater than 1 μm, and sometimes greater than 10 μm. The graphitic domains typically have a thickness from 1 nm to 200 nm, more typically from 1 nm to 100 nm, further more typically from 1 nm to 40 nm, and most typically from 1 nm to 30 nm.

Preferably, the solid graphene foam contains pores having a size from 0.5 nm to 50 nm. It may be noted that it has not been possible to use Ni-catalyzed CVD to produce graphene foams having a pore size range of 0.5-50 nm. This is due to the notion that it has not been proven possible to prepare Ni foam templates having such a pore size range and not possible for the hydrocarbon gas (precursor molecules) to readily enter Ni foam pores of these sizes. These Ni foam pores must also be interconnected. Additionally, the sacrificial plastic colloidal particle approaches have resulted in macro-pores that are in the size range of microns to millimeters.

In a preferred embodiment, the present invention provides a roll-to-roll process for producing a solid graphene foam composed of multiple pores and pore walls The process comprises: (a) preparing a graphene dispersion having a graphene material dispersed in a liquid medium, wherein the dispersion optionally contains a blowing agent; (b) continuously or intermittently dispensing and depositing the graphene dispersion onto a surface of a supporting substrate to form a continuous wet layer of graphene material under an orientation-inducing stress, wherein the supporting substrate is a continuous thin film supplied from a feeder roller and collected on a collector roller; (c) partially or completely removing the liquid medium from the wet layer of graphene material to form a continuous dried layer of graphene; (d) heat treating the dried layer of graphene material at a first heat treatment temperature from 100° C. to 1,500° C. at a desired heating rate sufficient to activate the blowing agent for producing a continuous layer of the solid graphene foam

having a density from 0.01 to 1.7 g/cm^3 or a specific surface area from 50 to 3,200 m^2/g; (e) impregnating the multiple pores with the liquid or gel electrolyte to form a continuous layer of pre-impregnated solid graphene foam, which is subjected to a step of compressing or roll-pressing that reduces a pore size, improve orientation of graphene planes, and squeeze excess electrolyte out of said pre-impregnated solid graphene foam for forming a continuous layer of the supercapacitor electrode; and (f) collecting the continuous layer of supercapacitor electrode on the collector roller. The electrode layer may be subjected to further heat treatments at a second temperature, higher than the first temperature, prior to electrolyte impregnation. The continuous or large-length layer of electrolyte-impregnated foam may be cut into smaller pieces and multiple pieces may be stacked to form a thicker electrode in a supercapacitor.

The orientation-inducing stress may be a shear stress. As an example, the shear stress can be encountered in a situation such as slot-die coating or reverse roll transfer coating. As another example, an effective orientation-inducing stress is created in an automated roll-to-roll coating process in which a "knife-on-roll" configuration dispenses the graphene dispersion over a moving solid substrate, such as a plastic film. The relative motion between this moving film and the coating knife acts to effect orientation of graphene sheets along the shear stress direction.

This orientation-inducing stress is a critically important step in the production of the presently invented graphene foams due to the surprising observation that the shear stress enables the graphene sheets to align along a particular direction (e.g. X-direction or length-direction) to produce preferred orientations and facilitate contacts between graphene sheets along foam walls. Further surprisingly, these preferred orientations and improved graphene-to-graphene contacts facilitate chemical merging or linking between graphene sheets during the subsequent heat treatment of the dried graphene layer. Such preferred orientations and improved contacts are essential to the eventual attainment of exceptionally high thermal conductivity, electrical conductivity, elastic modulus, and mechanical strength of the resulting graphene foam. In general, these great properties could not be obtained without such a shear stress-induced orientation control.

BRIEF DESCRIPTION OF THE DRAWINGS

FIG. 1(A) A flow chart illustrating various prior art processes of producing exfoliated graphite products (flexible graphite foils and expanded graphite flakes), along with a process for producing pristine graphene foam **40a** or graphene oxide foams **40b;**

FIG. 1(B) Schematic drawing illustrating the processes for producing conventional paper, mat, film, and membrane of simply aggregated graphite or NGP flakes/platelets. All processes begin with intercalation and/or oxidation treatment of graphitic materials (e.g. natural graphite particles).

FIG. 2 Schematic of a conventional supercapacitor cell.

FIG. 3 A possible mechanism of chemical linking between graphene oxide sheets that effectively increases the graphene sheet lateral dimensions.

FIG. 4(A) Thermal conductivity values vs. specific gravity of the GO suspension-derived foam produced by the presently invented process, meso-phase pitch-derived graphite foam, and Ni foam-template assisted CVD graphene foam;

FIG. 4(B) Thermal conductivity values of the GO suspension-derived foam, sacrificial plastic bead-templated GO foam, and the hydrothermally reduced GO graphene foam; and

FIG. 4(C) electrical conductivity data for the GO suspension-derived foam produced by the presently invented process and the hydrothermally reduced GO graphene foam.

FIG. 5(A) Thermal conductivity values (vs. specific gravity values up to 1.02 g/cm^3) of the GO suspension-derived foam, meso-phase pitch-derived graphite foam, and Ni foam-template assisted CVD graphene foam;

FIG. 5(B) Thermal conductivity values of the GO suspension-derived foam, sacrificial plastic bead-templated GO foam, and hydrothermally reduced GO graphene foam (vs. specific gravity values up to 1.02 g/cm^3).

FIG. 6 Thermal conductivity values of graphene foam samples derived from GO and GF (graphene fluoride) as a function of the specific gravity.

FIG. 7 Thermal conductivity values of graphene foam samples derived from GO and pristine graphene as a function of the final (maximum) heat treatment temperature.

FIG. 8(A) Inter-graphene plane spacing in graphene foam walls as measured by X-ray diffraction;

FIG. 8(B) The oxygen content in the GO suspension-derived graphene foam.

FIG. 9 The electrode specific capacitance values of two series of supercapacitors (conventional and presently invented) plotted as a function of the electrode density.

FIG. 10 Ragone plots (gravimetric and volumetric power density vs. energy density) of symmetric supercapacitor (EDLC) cells containing isolated nitrogen-doped graphene sheets or graphene foam as the electrode active material and EMIMBF4 ionic liquid electrolyte. Supercapacitors were prepared according to an embodiment of instant invention and, for comparison, by the conventional slurry coating of electrodes.

FIG. 11 Ragone plots of lithium ion capacitor (LIC) cells containing pristine graphene sheets as the electrode active material and lithium salt-PC/DEC organic liquid electrolyte. Supercapacitors were prepared according to an embodiment of instant invention and by the conventional slurry coating of electrodes.

FIG. 12 The cell-level gravimetric and volumetric energy densities plotted over the achievable electrode thickness range of the RGO-based EDLC supercapacitors (organic liquid electrolyte) prepared via the conventional method and the presently invented method. Legends: the gravimetric (♦) and volumetric (▲) energy density of the conventional supercapaitors (highest achieved electrode tap density of approximately 0.28 g/cm^3) and the gravimetric (■) and volumetric (x) energy density of the inventive supercapaitors (easily achieved electrode tap density of approximately 0.8 g/cm^3).

FIG. 13 The cell-level gravimetric energy densities plotted over the achievable active material proportion (active material weight/total cell weight) in a supercapacitor cell.

DESCRIPTION OF THE PREFERRED EMBODIMENTS

As schematically illustrated in FIG. 2, a prior art supercapacitor cell is typically composed of an anode current collector 202 (e.g. Al foil 12-15 μm thick), an anode active material (containing an anode active material, such as activated carbon particles 232 and conductive additives that are bonded by a resin binder, such as PVDF), a porous separator 230, a cathode active material layer 208 (containing a

cathode active material, such as activated carbon particles **234**, and conductive additives that are all bonded by a resin binder, not shown), a cathode current collector **206** (e.g. Al foil), and a liquid electrolyte disposed in both the anode active material layer **204** (also simply referred to as the "anode layer") and the cathode active material layer **208** (or simply "cathode layer"). The entire cell is encased in a protective housing, such as a thin plastic-aluminum foil laminate-based envelop. The prior art supercapacitor cell is typically made by a process that includes the following steps:

    a) The first step is mixing particles of the anode active material (e.g. activated carbon), a conductive filler (e.g. graphite flakes), a resin binder (e.g. PVDF) in a solvent (e.g. NMP) to form an anode slurry. On a separate basis, particles of the cathode active material (e.g. activated carbon), a conductive filler (e.g. acetylene black), a resin binder (e.g. PVDF) are mixed and dispersed in a solvent (e.g. NMP) to form a cathode slurry.

    b) The second step includes coating the anode slurry onto one or both primary surfaces of an anode current collector (e.g. Cu or Al foil), drying the coated layer by vaporizing the solvent (e.g. NMP) to form a dried anode electrode coated on Cu or Al foil. Similarly, the cathode slurry is coated and dried to form a dried cathode electrode coated on Al foil.

    c) The third step includes laminating an anode/Al foil sheet, a porous separator layer, and a cathode/Al foil sheet together to form a 3-layer or 5-layer assembly, which is cut and slit into desired sizes and stacked to form a rectangular structure (as an example of shape) or rolled into a cylindrical cell structure.

    d) The rectangular or cylindrical laminated structure is then encased in a laminated aluminum-plastic envelope or steel casing.

    e) A liquid electrolyte is then injected into the laminated housing structure to make a supercapacitor cell.

There are several serious problems associated with this conventional process and the resulting supercapacitor cell:

    1) It is very difficult to produce an electrode layer (anode layer or cathode layer) that is thicker than 100 μm and practically impossible or impractical to produce an electrode layer thicker than 200 μm. There are several reasons why this is the case. An electrode of 100 μm thickness typically requires a heating zone of 30-50 meters long in a slurry coating facility, which is too time consuming, too energy intensive, and not cost-effective. A heating zone longer than 100 meters is not unusual.

    2) For some electrode active materials, such as graphene sheets, it has not been possible to produce an electrode thicker than 50 μm in a real manufacturing environment on a continuous basis. This is despite the notion that some thicker electrodes have been claimed in open or patent literature, which were prepared in a laboratory on a small scale. In a laboratory setting, presumably one could repeatedly add new materials to a layer and manually consolidate the layer to increase the thickness of an electrode. However, even with such a procedure, the resulting electrode becomes very fragile and brittle. This is even worse for graphene-based electrodes, since repeated compressions lead to re-stacking of graphene sheets and, hence, significantly reduced specific surface area and reduced specific capacitance.

    3) With a conventional process, as depicted in FIG. **2**, the actual mass loadings of the electrodes and the apparent

densities for the active materials are too low. In most cases, the active material mass loadings of the electrodes (areal density) is significantly lower than 10 mg/cm² and the apparent volume density or tap density of the active material is typically less than 0.75 g/cm³ (more typically less than 0.5 g/cm³ and most typically less than 0.3 g/cm³) even for relatively large particles of activated carbon. In addition, there are so many other non-active materials (e.g. conductive additive and resin binder) that add additional weights and volumes to the electrode without contributing to the cell capacity. These low areal densities and low volume densities result in relatively low volumetric capacitances and low volumetric energy density.

    4) The conventional process requires dispersing electrode active materials (anode active material and cathode active material) in a liquid solvent (e.g. NMP) to make a wet slurry and, upon coating on a current collector surface, the liquid solvent has to be removed to dry the electrode layer. Once the anode and cathode layers, along with a separator layer, are laminated together and packaged in a housing to make a supercapacitor cell, one then injects a liquid electrolyte into the cell. In actuality, one makes the two electrodes wet, then makes the electrodes dry, and finally makes them wet again. Such a wet-dry-wet process is clearly not a good process at all.

    5) Current supercapacitors (e.g. symmetric supercapacitors or electric double layer capacitors, EDLC) still suffer from a relatively low gravimetric energy density and low volumetric energy density. Commercially available EDLCs exhibit a gravimetric energy density of approximately 6 Wh/kg and no experimental EDLC cells have been reported to exhibit an energy density higher than 10 Wh/kg (based on the total cell weight) at room temperature. Although experimental supercapacitors exhibit large volumetric electrode capacitances (100 to 200 F/cm³ in most cases) at the electrode level (not the cell level), their typical active mass loading of <1 mg/cm², tap density of <0.1 g/cm³, and electrode thicknesses of up to tens of micrometers remain significantly lower than those used in most commercially available electrochemical capacitors, resulting in energy storage devices with relatively low areal and volumetric capacities and low volumetric energy densities based on the cell (device) weight.

In literature, the energy density data reported based on either the active material weight alone or electrode weight cannot directly translate into the energy densities of a practical supercapacitor cell or device. The "overhead weight" or weights of other device components (binder, conductive additive, current collectors, separator, electrolyte, and packaging) must also be taken into account. The convention production process results in an active material proportion being less than 30% by weight of the total cell weight (<15% in some cases; e.g. for graphene-based active material).

The present invention provides a process for producing a supercapacitor cell having a high electrode thickness (no theoretical limitation on the electrode thickness that can be made by using the present process), high active material mass loading, low overhead weight and volume, high volumetric capacitance, and high volumetric energy density. The electrode produced can be directly impregnated with an electrolyte (aqueous, organic, ionic liquid, or polymer gel) without going through the lengthy and environmentally unfriendly wet-dry-wet procedures of the prior art process.

In some preferred embodiments, the present invention provides a supercapacitor electrode comprising a solid graphene foam impregnated with a liquid or gel electrolyte, wherein the solid graphene foam is composed of multiple pores and pore walls, wherein the pore walls contain a pristine graphene material having essentially zero % of non-carbon elements, or a non-pristine graphene material having 0.001% to 5% by weight of non-carbon elements wherein the non-pristine graphene is selected from graphene oxide, reduced graphene oxide, graphene fluoride, graphene chloride, graphene bromide, graphene iodide, hydrogenated graphene, nitrogenated graphene, doped graphene, chemically functionalized graphene, doped graphene, or a combination thereof, and the solid graphene foam, when measured in a dried state without said electrolyte, has a physical density from 0.01 to 1.7 g/cm^3, a specific surface area from 50 to 3,300 m^2/g, a thermal conductivity of at least 200 W/mK per unit of specific gravity, and/or an electrical conductivity no less than 2,000 S/cm per unit of specific gravity. The pore walls preferably and typically contain stacked graphene planes having an inter-plane spacing d_{002} from 0.3354 nm to 0.40 nm as measured by X-ray diffraction.

In certain preferred embodiments, the present invention provides a sheet of solid graphene foam composed of multiple pores and pore walls, which are then impregnated with an electrolyte. The pores in the graphene foam are formed slightly before, during, or after sheets of a graphene material are (1) chemically linked/merged together (edge-to-edge and/or face-to-face) typically at a temperature from 100 to 1,500° C. and/or (2) re-organized into larger graphite crystals or domains (herein referred to as re-graphitization) along the pore walls at a high temperature (typically >2,100° C. and more typically >2,500° C.). Optionally, the electrolyte-impregnated graphene foam is then compressed or roll-pressed to improve the wetting of graphene walls by the liquid or gel electrolyte, squeeze out excess electrolyte, and reduce the pore sizes or separation between graphene sheets for enhanced tap density.

In a preferred embodiment, the process comprises:

(a) preparing a graphene dispersion having a graphene material dispersed in a liquid medium, wherein the graphene material is selected from pristine graphene, graphene oxide, reduced graphene oxide, graphene fluoride, graphene chloride, graphene bromide, graphene iodide, hydrogenated graphene, nitrogenated graphene, chemically functionalized graphene, doped graphene, or a combination thereof and wherein the dispersion contains an optional blowing agent with a blowing agent-to-graphene material weight ratio from 0/1.0 to 1.0/1.0 (this blowing agent is normally required if the graphene material is pristine graphene, typically having a blowing agent-to-pristine graphene weight ratio from 0.01/1.0 to 1.0/1.0);

(b) dispensing and depositing the graphene dispersion onto a surface of a supporting substrate (e.g. plastic film, rubber sheet, metal foil, glass sheet, paper sheet, etc.) to form a first wet layer of graphene material, wherein the dispensing and depositing procedure (e.g. coating or casting) includes subjecting the graphene dispersion to an orientation-inducing stress (preferably entailing a shear stress);

(c) partially or completely removing the liquid medium from the first wet layer of graphene material to form a first dried layer of graphene material having a content of non-carbon elements (e.g. O, H, N, B, F, Cl, Br, I, etc.) no less than 5% by weight (this non-carbon content, when being removed via heat-induced decomposition, produces volatile gases that act as a foaming agent or blowing agent);

(d) heat treating the first layer of graphene material at a first heat treatment temperature from 100° C. to 3,000° C. at a desired heating rate sufficient to induce volatile gas molecules from the non-carbon elements or to activate said blowing agent for producing the solid graphene foam. The graphene foam typically has a density from 0.01 to 1.7 g/cm^3 (more typically from 0.1 to 1.5 g/cm^3, and even more typically from 0.3 to 1.3 g/cm^3, and most typically from 0.5 to 1.1 g/cm^3), or a specific surface area from 50 to 3,200 m^2/g (more typically from 200 to 2,800 m^2/g, and most typically from 500 to 2,500 m^2/g). Optionally, the specific surface area can be further increased by subjecting the graphene foam to a chemical or physical activation treatment (e.g. mixing with KOH at **700–900**° C. for 2-6 hours).

(e) impregnating the pores of graphene foam with a liquid or gel electrolyte to form electrolyte-impregnated graphene foam, which is then optionally compressed (e.g. roll-pressed) to increase the tap density of the foam.

A blowing agent or foaming agent is a substance which is capable of producing a cellular or foamed structure via a foaming process in a variety of materials that undergo hardening or phase transition, such as polymers (plastics and rubbers), glass, and metals. They are typically applied when the material being foamed is in a liquid state. It has not been previously known that a blowing agent can be used to create a foamed material while in a solid state. More significantly, it has not been taught or hinted that an aggregate of sheets of a graphene material can be converted into a graphene foam via a blowing agent. The cellular structure in a matrix is typically created for the purpose of reducing density, increasing thermal resistance and acoustic insulation, while increasing the thickness and relative stiffness of the original polymer.

Blowing agents or related foaming mechanisms to create pores or cells (bubbles) in a matrix for producing a foamed or cellular material, can be classified into the following groups:

(a) Physical blowing agents: e.g. hydrocarbons (e.g. pentane, isopentane, cyclopentane), chlorofluorocarbons (CFCs), hydrochlorofluorocarbons (HCFCs), and liquid CO_2. The bubble/foam-producing process is endothermic, i.e. it needs heat (e.g. from a melt process or the chemical exotherm due to cross-linking), to volatize a liquid blowing agent.

(b) Chemical blowing agents: e.g. isocyanate, azo-, hydrazine and other nitrogen-based materials (for thermoplastic and elastomeric foams), sodium bicarbonate (e.g. baking soda, used in thermoplastic foams). Here gaseous products and other by-products are formed by a chemical reaction, promoted by process or a reacting polymer's exothermic heat. Since the blowing reaction involves forming low molecular weight compounds that act as the blowing gas, additional exothermic heat is also released. Powdered titanium hydride is used as a foaming agent in the production of metal foams, as it decomposes to form titanium and hydrogen gas at elevated temperatures. Zirconium (II) hydride is used for the same purpose. Once formed the low molecular weight compounds will never revert to the original blowing agent(s), i.e. the reaction is irreversible.

(c) Mixed physical/chemical blowing agents: e.g. used to produce flexible polyurethane (PU) foams with very low densities. Both the chemical and physical blowing can be used in tandem to balance each other out with respect to thermal energy released/absorbed; hence, minimizing temperature rise. For instance, isocyanate and water (which react to form CO_2) are used in

combination with liquid CO_2 (which boils to give gaseous form) in the production of very low density flexible PU foams for mattresses.

(d) Mechanically injected agents: Mechanically made foams involve methods of introducing bubbles into liquid polymerizable matrices (e.g. an unvulcanized elastomer in the form of a liquid latex). Methods include whisking-in air or other gases or low boiling volatile liquids in low viscosity lattices, or the injection of a gas into an extruder barrel or a die, or into injection molding barrels or nozzles and allowing the shear/mix action of the screw to disperse the gas uniformly to form very fine bubbles or a solution of gas in the melt. When the melt is molded or extruded and the part is at atmospheric pressure, the gas comes out of solution expanding the polymer melt immediately before solidification.

(e) Soluble and leachable agents: Soluble fillers, e.g. solid sodium chloride crystals mixed into a liquid urethane system, which is then shaped into a solid polymer part, the sodium chloride is later washed out by immersing the solid molded part in water for some time, to leave small inter-connected holes in relatively high density polymer products.

(f) We have found that the above five mechanisms can all be used to create pores in the graphene materials while they are in a solid state. Another mechanism of producing pores in a graphene material is through the generation and vaporization of volatile gases by removing those non-carbon elements in a high-temperature environment. This is a unique self-foaming process that has never been previously taught or suggested.

In a preferred embodiment, the graphene material in the dispersion is selected from pristine graphene, graphene oxide, reduced graphene oxide, graphene fluoride, graphene chloride, graphene bromide, graphene iodide, hydrogenated graphene, nitrogenated graphene, chemically functionalized graphene, doped graphene, or a combination thereof. The starting graphitic material for producing any one of the above graphene materials may be selected from natural graphite, artificial graphite, meso-phase carbon, meso-phase pitch, meso-carbon micro-bead, soft carbon, hard carbon, coke, carbon fiber, carbon nano-fiber, carbon nano-tube, or a combination thereof.

For instance, the graphene oxide (GO) may be obtained by immersing powders or filaments of a starting graphitic material (e.g. natural graphite powder) in an oxidizing liquid medium (e.g. a mixture of sulfuric acid, nitric acid, and potassium permanganate) in a reaction vessel at a desired temperature for a period of time (typically from 0.5 to 96 hours, depending upon the nature of the starting material and the type of oxidizing agent used). The resulting graphite oxide particles may then be subjected to thermal exfoliation or ultrasonic wave-induced exfoliation to produce GO sheets.

Pristine graphene may be produced by direct ultrasonication (also known as liquid phase production) or supercritical fluid exfoliation of graphite particles. These processes are well-known in the art. Multiple pristine graphene sheets may be dispersed in water or other liquid medium with the assistance of a surfactant to form a suspension. A chemical blowing agent may then be dispersed into the dispersion (**38** in FIG. **1**(A)). This suspension is then cast or coated onto the surface of a solid substrate (e.g. glass sheet or Al foil). When heated to a desired temperature, the chemical blowing agent is activated or decomposed to generate volatile gases (e.g.

N_2 or CO_2), which act to form bubbles or pores in an otherwise mass of solid graphene sheets, forming a pristine graphene foam **40***a*.

Fluorinated graphene or graphene fluoride is herein used as an example of the halogenated graphene material group. There are two different approaches that have been followed to produce fluorinated graphene: (1) fluorination of pre-synthesized graphene: This approach entails treating graphene prepared by mechanical exfoliation or by CVD growth with fluorinating agent such as XeF_2, or F-based plasmas; (2) Exfoliation of multilayered graphite fluorides: Both mechanical exfoliation and liquid phase exfoliation of graphite fluoride can be readily accomplished [F. Karlicky, et al. "*Halogenated Graphenes: Rapidly Growing Family of Graphene Derivatives*" ACS Nano, 2013, 7 (8), pp 6434-6464].

Interaction of F_2 with graphite at high temperature leads to covalent graphite fluorides $(CF)_n$ or $(C_2F)_n$, while at low temperatures graphite intercalation compounds (GIC) C_xF ($2 \le x \le 24$) form. In $(CF)_n$ carbon atoms are sp3-hybridized and thus the fluorocarbon layers are corrugated consisting of trans-linked cyclohexane chairs. In $(C_2F)_n$ only half of the C atoms are fluorinated and every pair of the adjacent carbon sheets are linked together by covalent C—C bonds. Systematic studies on the fluorination reaction showed that the resulting F/C ratio is largely dependent on the fluorination temperature, the partial pressure of the fluorine in the fluorinating gas, and physical characteristics of the graphite precursor, including the degree of graphitization, particle size, and specific surface area. In addition to fluorine (F_2), other fluorinating agents may be used, although most of the available literature involves fluorination with F_2 gas, sometimes in presence of fluorides.

For exfoliating a layered precursor material to the state of individual layers or few-layers, it is necessary to overcome the attractive forces between adjacent layers and to further stabilize the layers. This may be achieved by either covalent modification of the graphene surface by functional groups or by non-covalent modification using specific solvents, surfactants, polymers, or donor-acceptor aromatic molecules. The process of liquid phase exfoliation includes ultrasonic treatment of a graphite fluoride in a liquid medium.

The nitrogenation of graphene can be conducted by exposing a graphene material, such as graphene oxide, to ammonia at high temperatures (200-400° C.). Nitrogenated graphene could also be formed at lower temperatures by a hydrothermal method; e.g. by sealing GO and ammonia in an autoclave and then increased the temperature to 150-250° C. Other methods to synthesize nitrogen doped graphene include nitrogen plasma treatment on graphene, arc-discharge between graphite electrodes in the presence of ammonia, ammonolysis of graphene oxide under CVD conditions, and hydrothermal treatment of graphene oxide and urea at different temperatures.

The pore walls (cell walls) in the presently invented graphene foam contain chemically bonded and merged graphene planes. These planar aromatic molecules or graphene planes (hexagonal structured carbon atoms) are well interconnected physically and chemically. The lateral dimensions (length or width) of these planes are huge (from 20 nm to >10 μm), typically several times or even orders of magnitude larger than the maximum crystallite dimension (or maximum constituent graphene plane dimension) of the starting graphite particles. The graphene sheets or planes are essentially interconnected to form electron-conducting pathways with low resistance. This is a unique and new class of

material that has not been previously discovered, developed, or suggested to possibly exist.

In order to illustrate how the presently invented process works to produce a graphene foam, we herein make use of graphene oxide (GO) and graphene fluoride (GF) as two examples. These should not be construed as limiting the scope of our claims. In each case, the first step involves preparation of a graphene dispersion (e.g. GO+water or GF+organic solvent, DMF) containing an optional blowing agent. If the graphene material is pristine graphene containing no non-carbon elements, a blowing agent is required.

In step (b), the GF or GO suspension (**21** in FIG. **1**(A)) is formed into a wet GF or GO layer **35** on a solid substrate surface (e.g. PET film or glass) preferably under the influence of a shear stress. One example of such a shearing procedure is casting or coating a thin film of GF or GO suspension using a coating machine. This procedure is similar to a layer of varnish, paint, coating, or ink being coated onto a solid substrate. The roller, "doctor's blade", or wiper creates a shear stress when the film is shaped, or when there is a relative motion between the roller/blade/wiper and the supporting substrate. Quite unexpectedly and significantly, such a shearing action enables the planar GF or GO sheets to well align along, for instance, a shearing direction. Further surprisingly, such a molecular alignment state or preferred orientation is not disrupted when the liquid components in the GF or GO suspension are subsequently removed to form a well-packed layer of highly aligned GF or GO sheets that are at least partially dried. The dried GF or GO mass **37**a has a high birefringence coefficient between an in-plane direction and the normal-to-plane direction.

In an embodiment, this GF or GO layer is then subjected to a heat treatment to activate the blowing agent and/or the thermally-induced reactions that remove the non-carbon elements (e.g. F, O, etc.) from the graphene sheets to generate volatile gases as by-products. These volatile gases generate pores or bubbles inside the solid graphene material, pushing solid graphene sheets into a wall structure, forming a graphene oxide foam **40**b. If no blowing agent is added, the non-carbon elements in the graphene material preferably occupy at least 10% by weight of the graphene material (preferably at least 20%, and further preferably at least 30%). The first (initial) heat treatment temperature is typically greater than 80° C., preferably greater than 100° C., more preferably greater than 300° C., further more preferably greater than 500° C. and can be as high as 1,500° C. The blowing agent is typically activated at a temperature from 80° C. to 300° C., but can be higher. The foaming procedure (formation of pores, cells, or bubbles) is typically completed within the temperature range of 80-1,500° C. Quite surprisingly, the chemical linking or merging between graphene planes (GO or GF planes) in an edge-to-edge and face-to-face manner can occur at a relatively low heat treatment temperature (e.g. as low as from 150 to 300° C.).

The foamed graphene material may be subjected to a further heat treatment that involves at least a second temperature that is significantly higher than the first heat treatment temperature.

A properly programmed heat treatment procedure can involve just a single heat treatment temperature (e.g. a first heat treatment temperature only), at least two heat treatment temperatures (first temperature for a period of time and then raised to a second temperature and maintained at this second temperature for another period of time), or any other combination of heat treatment temperatures (HTT) that involve an initial treatment temperature (first temperature) and a fmal HTT (second), higher than the first. The highest or final

HTT that the dried graphene layer experiences may be divided into four distinct HTT regimes:

Regime 1 (80° C. to 300° C.): In this temperature range (the thermal reduction regime and also the activation regime for a blowing agent, if present), a GO or GF layer primarily undergoes thermally-induced reduction reactions, leading to a reduction of oxygen content or fluorine content from typically 20-50% (of O in GO) or 10-25% (of F in GF) to approximately 5-6%. This treatment results in a reduction of inter-graphene spacing in foam walls from approximately 0.6-1.2 nm (as dried) down to approximately 0.4 nm, and an increase in thermal conductivity to 200 W/mK per unit specific gravity and/or electrical conductivity to 2,000 S/cm per unit of specific gravity. (Since one can vary the level of porosity and, hence, specific gravity of a graphene foam material and, given the same graphene material, both the thermal conductivity and electric conductivity values vary with the specific gravity, these property values must be divided by the specific gravity to facilitate a fair comparison.) Even with such a low temperature range, some chemical linking between graphene sheets occurs. The inter-GO or inter-GF planar spacing remains relatively large (0.4 nm or larger). Many O- or F-containing functional groups survive.

Regime 2 (300° C.-1,500° C.): In this chemical linking regime, extensive chemical combination, polymerization, and cross-linking between adjacent GO or GF sheets occur. The oxygen or fluorine content is reduced to typically <1.0% (e.g. 0.7%) after chemical linking, resulting in a reduction of inter-graphene spacing to approximately 0.345 nm. This implies that some initial re-graphitization has already begun at such a low temperature, in stark contrast to conventional graphitizable materials (such as carbonized polyimide film) that typically require a temperature as high as 2,500° C. to initiate graphitization. This is another distinct feature of the presently invented graphene foam and its production processes. These chemical linking reactions result in an increase in thermal conductivity to 250 W/mK per unit of specific gravity, and/or electrical conductivity to 2,500-4,000 S/cm per unit of specific gravity.

Regime 3 (1,500-2,500° C.): In this ordering and re-graphitization regime, extensive graphitization or graphene plane merging occurs, leading to significantly improved degree of structural ordering in the foam walls. As a result, the oxygen or fluorine content is reduced to typically 0.01% and the inter-graphene spacing to approximately 0.337 nm (achieving degree of graphitization from 1% to approximately 80%, depending upon the actual HTT and length of time). The improved degree of ordering is also reflected by an increase in thermal conductivity to >350 W/mK per unit of specific gravity, and/or electrical conductivity to >3,500 S/cm per unit of specific gravity.

Regime 4 (higher than 2,500° C.): In this re-crystallization and perfection regime, extensive movement and elimination of grain boundaries and other defects occur, resulting in the formation of nearly perfect single crystals or poly-crystalline graphene crystals with huge grains in the foam walls, which can be orders of magnitude larger than the original grain sizes of the starting graphite particles for the production of GO or GF. The oxygen or fluorine content is essentially eliminated, typically 0%—0.001%. The inter-graphene spacing is reduced to down to approximately 0.3354 nm (degree of graphitization from 80% to nearly 100%), corresponding to that of a perfect

graphite single crystal. The foamed structure thus obtained exhibits a thermal conductivity of >400'W/mK per unit of specific gravity, and electrical conductivity of >4,000 S/cm per unit of specific gravity.

The presently invented graphene foam structure can be obtained by heat-treating the dried GO or GF layer with a temperature program that covers at least the first regime (typically requiring 1-4 hours in this temperature range if the temperature never exceeds 500° C.), more commonly covers the first two regimes (1-2 hours preferred), still more commonly the first three regimes (preferably 0.5-2.0 hours in Regime 3), and can cover all the 4 regimes (including Regime 4 for 0.2 to 1 hour, may be implemented to achieve the highest conductivity).

If the graphene material is selected from the group of non-pristine graphene materials consisting of graphene oxide, reduced graphene oxide, graphene fluoride, graphene chloride, graphene bromide, graphene iodide, hydrogenated graphene, nitrogenated graphene, chemically functionalized graphene, doped graphene, or a combination thereof, and wherein the maximum heat treatment temperature (e.g. both the first and second heat treatment temperatures) is (are) less than 2,500° C., then the resulting solid graphene foam typically contains a content of non-carbon elements in the range of 0.01% to 2.0% by weight (non-pristine graphene foam).

X-ray diffraction patterns were obtained with an X-ray diffractometer equipped with CuKcv radiation. The shift and broadening of diffraction peaks were calibrated using a silicon powder standard. The degree of graphitization, g, was calculated from the X-ray pattern using the Mering's Eq, $d_{002}=0.3354$ g$+0.344$ $(1-g)$, where d_{002} is the interlayer spacing of graphite or graphene crystal in nm. This equation is valid only when d_{002} is equal or less than approximately 0.3440 nm. The graphene foam walls having a d_{002} higher than 0.3440 nm reflects the presence of oxygen- or fluorine-containing functional groups (such as —F, —OH, >O, and —COOH on graphene molecular plane surfaces or edges) that act as a spacer to increase the inter-graphene spacing.

Another structural index that can be used to characterize the degree of ordering of the stacked and bonded graphene planes in the foam walls of graphene and conventional graphite crystals is the "mosaic spread," which is expressed by the full width at half maximum of a rocking curve (X-ray diffraction intensity) of the (002) or (004) reflection. This degree of ordering characterizes the graphite or graphene crystal size (or grain size), amounts of grain boundaries and other defects, and the degree of preferred grain orientation. A nearly perfect single crystal of graphite is characterized by having a mosaic spread value of 0.2-0.4. Most of our graphene walls have a mosaic spread value in this range of 0.2-0.4 (if produced with a heat treatment temperature (HTT) no less than 2,500° C.). However, some values are in the range of 0.4-0.7 if the HTT is between 1,500 and 2,500° C., and in the range of 0.7-1.0 if the HTT is between 300 and 1,500° C.

Illustrated in FIG. **3** is a plausible chemical linking mechanism where only 2 aligned GO molecules are shown as an example, although a large number of GO molecules can be chemically linked together to form a foam wall. Further, chemical linking could also occur face-to-face, not just edge-to-edge for GO, GF, and chemically functionalized graphene sheets. These linking and merging reactions proceed in such a manner that the molecules are chemically merged, linked, and integrated into one single entity. The graphene sheets (GO or GF sheets) completely lose their own original identity and they no longer are discrete sheets/

platelets/flakes. The resulting product is not a simple aggregate of individual graphene sheets, but a single entity that is essentially a network of interconnected giant molecules with an essentially infinite molecular weight. This may also be described as a graphene poly-crystal (with several grains, but typically no discernible, well-defined grain boundaries). All the constituent graphene planes are very large in lateral dimensions (length and width) and, if the HTT is sufficiently high (e.g. >1,500° C. or much higher), these graphene planes are essentially bonded together with one another.

In-depth studies using a combination of SEM, TEM, selected area diffraction, X-ray diffraction, AFM, Raman spectroscopy, and FTIR indicate that the graphene foam walls are composed of several huge graphene planes (with length/width typically >>20 nm, more typically >>100 nm, often >>1 μm, and, in many cases, >>10 μm, or even >>100 μm). These giant graphene planes are stacked and bonded along the thickness direction (crystallographic c-axis direction) often through not just the van der Waals forces (as in conventional graphite crystallites), but also covalent bonds, if the final heat treatment temperature is lower than 2,500° C. In these cases, wishing not to be limited by theory, but Raman and FTIR spectroscopy studies appear to indicate the co-existence of sp^2 (dominating) and sp^3 (weak but existing) electronic configurations, not just the conventional sp^2 in graphite.

(1) This graphene foam wall is not made by gluing or bonding discrete flakes/platelets together with a resin binder, linker, or adhesive. Instead, GO sheets (molecules) from the GO dispersion or the GF sheets from the GF dispersion are merged through joining or forming of covalent bonds with one another, into an integrated graphene entity, without using any externally added linker or binder molecules or polymers.

(2) This graphene foam wall is typically a poly-crystal composed of large grains having incomplete grain boundaries. This entity is derived from a GO or GF suspension, which is in turn obtained from natural graphite or artificial graphite particles originally having multiple graphite crystallites. Prior to being chemically oxidized or fluorinated, these starting graphite crystallites have an initial length (L_a in the crystallographic a-axis direction), initial width (L_b in the b-axis direction), and thickness (L_c in the c-axis direction). Upon oxidation or fluorination, these initially discrete graphite particles are chemically transformed into highly aromatic graphene oxide or graphene fluoride molecules having a significant concentration of edge- or surface-borne functional groups (e.g. —F, —OH, —COOH, etc.). These aromatic GO or GF molecules in the suspension have lost their original identity of being part of a graphite particle or flake. Upon removal of the liquid component from the suspension, the resulting GO or GF molecules form an essentially amorphous structure. Upon heat treatments, these GO or GF molecules are chemically merged and linked into a unitary or monolithic graphene entity that constitutes the foam wall. This foam wall is highly ordered.

The resulting unitary graphene entity in the foam wall typically has a length or width significantly greater than the L_a and L_b of the original crystallites. The length/width of this graphene foam wall entity is significantly greater than the L_a and L_b of the original crystallites. Even the individual grains in a poly-crystalline graphene wall structure have a length or width significantly greater than the L_a and L_b of the original crystallites.

(3) Due to these unique chemical composition (including oxygen or fluorine content), morphology, crystal structure

(including inter-graphene spacing), and structural features (e.g. high degree of orientations, few defects, incomplete grain boundaries, chemical bonding and no gap between graphene sheets, and substantially no interruptions in graphene planes), the GO- or GF-derived graphene foam has a unique combination of outstanding thermal conductivity, electrical conductivity, mechanical strength, and stiffness (elastic modulus).

The aforementioned features are further described and explained in detail as follows: As illustrated in FIG. 1(B), a graphite particle (e.g. **100**) is typically composed of multiple graphite crystallites or grains. A graphite crystallite is made up of layer planes of hexagonal networks of carbon atoms. These layer planes of hexagonally arranged carbon atoms are substantially flat and are oriented or ordered so as to be substantially parallel and equidistant to one another in a particular crystallite. These layers of hexagonal-structured carbon atoms, commonly referred to as graphene layers or basal planes, are weakly bonded together in their thickness direction (crystallographic c-axis direction) by weak van der Waals forces and groups of these graphene layers are arranged in crystallites. The graphite crystallite structure is usually characterized in terms of two axes or directions: the c-axis direction and the a-axis (or b-axis) direction. The c-axis is the direction perpendicular to the basal planes. The a- or b-axes are the directions parallel to the basal planes (perpendicular to the c-axis direction).

A highly ordered graphite particle can consist of crystallites of a considerable size, having a length of L_a along the crystallographic a-axis direction, a width of L_b along the crystallographic b-axis direction, and a thickness L_c along the crystallographic c-axis direction. The constituent graphene planes of a crystallite are highly aligned or oriented with respect to each other and, hence, these anisotropic structures give rise to many properties that are highly directional. For instance, the thermal and electrical conductivity of a crystallite are of great magnitude along the plane directions (a- or b-axis directions), but relatively low in the perpendicular direction (c-axis). As illustrated in the upper-left portion of FIG. 1(B), different crystallites in a graphite particle are typically oriented in different directions and, hence, a particular property of a multi-crystallite graphite particle is the directional average value of all the constituent crystallites.

Due to the weak van der Waals forces holding the parallel graphene layers, natural graphite can be treated so that the spacing between the graphene layers can be appreciably opened up so as to provide a marked expansion in the c-axis direction, and thus form an expanded graphite structure in which the laminar character of the carbon layers is substantially retained. The process for manufacturing flexible graphite is well-known in the art. In general, flakes of natural graphite (e.g. **100** in FIG. 1(B)) are intercalated in an acid solution to produce graphite intercalation compounds (GICs, **102**). The GICs are washed, dried, and then exfoliated by exposure to a high temperature for a short period of time. This causes the flakes to expand or exfoliate in the c-axis direction of the graphite up to 80-300 times of their original dimensions. The exfoliated graphite flakes are vermiform in appearance and, hence, are commonly referred to as worms **104**. These worms of graphite flakes which have been greatly expanded can be formed without the use of a binder into cohesive or integrated sheets of expanded graphite, e.g. webs, papers, strips, tapes, foils, mats or the like (typically referred to as "flexible graphite" **106**) having a typical density of about 0.04-2.0 g/cm³ for most applications.

The upper left portion of FIG. 1(A) shows a flow chart that illustrates the prior art processes used to fabricate flexible graphite foils. The processes typically begin with intercalating graphite particles **20** (e.g., natural graphite or synthetic graphite) with an intercalant (typically a strong acid or acid mixture) to obtain a graphite intercalation compound **22** (GIC). After rinsing in water to remove excess acid, the GIC becomes "expandable graphite." The GIC or expandable graphite is then exposed to a high temperature environment (e.g., in a tube furnace preset at a temperature in the range of 800-1,050° C.) for a short duration of time (typically from 15 seconds to 2 minutes). This thermal treatment allows the graphite to expand in its c-axis direction by a factor of 30 to several hundreds to obtain a worm-like vermicular structure **24** (graphite worm), which contains exfoliated, but un-separated graphite flakes with large pores interposed between these interconnected flakes.

In one prior art process, the exfoliated graphite (or mass of graphite worms) is re-compressed by using a calendaring or roll-pressing technique to obtain flexible graphite foils (**26** in FIG. 1(A) or **106** in FIG. 1(B)), which are typically 100-300 μm thick. In another prior art process, the exfoliated graphite worm **24** may be impregnated with a resin and then compressed and cured to form a flexible graphite composite, which is normally of low strength as well. In addition, upon resin impregnation, the electrical and thermal conductivity of the graphite worms could be reduced by two orders of magnitude.

Alternatively, the exfoliated graphite may be subjected to high-intensity mechanical shearing/separation treatments using a high-intensity air jet mill, high-intensity ball mill, or ultrasonic device to produce separated nano graphene platelets **33** (NGPs) with all the graphene platelets thinner than 100 nm, mostly thinner than 10 nm, and, in many cases, being single-layer graphene (also illustrated as **112** in FIG. 1(B)). An NGP is composed of a graphene sheet or a plurality of graphene sheets with each sheet being a two-dimensional, hexagonal structure of carbon atoms. A mass of multiple NGPs (including discrete sheets/platelets of single-layer and/or few-layer graphene or graphene oxide, **33** in FIG. 1(A)) may be made into a graphene film/paper (**34** in FIG. 1(A) or **114** in FIG. 1(B)) using a film- or paper-making process.

Further alternatively, with a low-intensity shearing, graphite worms tend to be separated into the so-called expanded graphite flakes (**108** in FIG. 1(B) having a thickness >100 nm. These flakes can be formed into graphite paper or mat **106** using a paper- or mat-making process. This expanded graphite paper or mat **106** is just a simple aggregate or stack of discrete flakes having defects, interruptions, and mis-orientations between these discrete flakes.

The solid graphene foam produced by the presently invented process may be further subjected to the following treatments, separately or in combination:

    (a) Being chemically functionalized or doped with atomic, ionic, or molecular species. Useful surface functional groups may include quinone, hydroquinone, quaternized aromatic amines, mercaptans, or disulfides. This class of functional groups can impart pseudo-capacitance to graphene-based supercapacitors.

    (b) coated or grafted with an intrinsically conductive polymer (conducting polymers, such as polyacetylene, polypyrrole, polyaniline, polythiophene, and their derivatives, are good choices for use in the present invention); These treatments are intended for further increasing the capacitance value through pseudo-capacitance effects such as redox reactions.

(c) deposition with transition metal oxides or sulfides, such as RuO_2, TiO_2, MnO_2, Cr_2O_3, and Co_2O_3, for the purpose of forming redox pairs with graphene sheets, thereby imparting pseudo-capacitance to the electrode; and

(d) subjected to an activation treatment (analogous to activation of carbon black materials) to create additional surfaces and possibly imparting functional chemical groups to these surfaces. The activation treatment can be accomplished through CO_2 physical activation, KOH chemical activation, or exposure to nitric acid, fluorine, or ammonia plasma.

In the instant invention, there is no limitation on the type of liquid or gel electrolytes that can be used in the supercapacitor: aqueous, organic, gel, and ionic liquid. Typically, electrolytes for supercapacitors consist of solvent and dissolved chemicals (e.g. salts) that dissociate into positive ions (cations) and negative ions (anions), making the electrolyte electrically conductive. The more ions the electrolyte contains, the better its conductivity, which also influences the capacitance. In supercapacitors, the electrolyte provides the molecules for the separating monolayer in the Helmholtz double-layer (electric double layer) and delivers the ions for pseudocapacitance.

Water is a relatively good solvent for dissolving inorganic chemicals. When added together with acids such as sulfuric acid (H_2SO_4), alkalis such as potassium hydroxide (KOH), or salts such as quaternary phosphonium salts, sodium perchlorate ($NaClO_4$), lithium perchlorate ($LiClO_4$) or lithium hexafluoride arsenate ($LiAsF_6$), water offers relatively high conductivity values. Aqueous electrolytes have a dissociation voltage of 1.15 V per electrode and a relatively low operating temperature range. Water electrolyte-based supercapacitors exhibit low energy density.

Alternatively, electrolytes may contain organic solvents, such as acetonitrile, propylene carbonate, tetrahydrofuran, diethyl carbonate, γ-butyrolactone, and solutes with quaternary ammonium salts or alkyl ammonium salts such as tetraethylammonium tetrafluoroborate ($N(Et)_4BF_4$) or triethyl (methyl) tetrafluoroborate ($NMe(Et)_3BF_4$). Organic electrolytes are more expensive than aqueous electrolytes, but they have a higher dissociation voltage of typically 1.35 V per electrode (2.7 V capacitor voltage), and a higher temperature range. The lower electrical conductivity of organic solvents (10 to 60 mS/cm) leads to a lower power density, but a higher energy density since the energy density is proportional to the square of the voltage.

The ionic liquid is composed of ions only. Ionic liquids are low melting temperature salts that are in a molten or liquid state when above a desired temperature. For instance, a salt is considered as an ionic liquid if its melting point is below 100° C. If the melting temperature is equal to or lower than room temperature (25° C.), the salt is referred to as a room temperature ionic liquid (RTIL). The IL salts are characterized by weak interactions, due to the combination of a large cation and a charge-delocalized anion. This results in a low tendency to crystallize due to flexibility (anion) and asymmetry (cation).

A typical and well-known ionic liquid is formed by the combination of a 1-ethyl-3-methylimidazolium (EMI) cation and an N,N-bis(trifluoromethane)sulphonamide (TFSI) anion. This combination gives a fluid with an ionic conductivity comparable to many organic electrolyte solutions and a low decomposition propensity and low vapor pressure up to −300-400° C. This implies a generally low volatility and non-flammability and, hence, a much safer electrolyte for batteries.

Ionic liquids are basically composed of organic ions that come in an essentially unlimited number of structural variations owing to the preparation ease of a large variety of their components. Thus, various kinds of salts can be used to design the ionic liquid that has the desired properties for a given application. These include, among others, imidazolium, pyrrolidinium and quaternary ammonium salts as cations and bis(trifluoromethanesulphonyl) imide, bis(fluorosulphonyl)imide, and hexafluorophosphate as anions. Based on their compositions, ionic liquids come in different classes that basically include aprotic, protic and zwitterionic types, each one suitable for a specific application.

Common cations of room temperature ionic liquids (RTILs) include, but not limited to, tetraalkylammonium, di-, tri-, and tetra-alkylimidazolium, alkylpyridinium, dialkyl-pyrrolidinium, dialkylpiperidinium, tetraalkylphosphonium, and trialkylsulfonium. Common anions of RTILs include, but not limited to, BF_4^-, $B(CN)_4^-$, $CH_3BF_3^-$, $CH2CHBF_3^-$, $CF_3BF_3^-$, $C_2F_5BF_3^-$, $n-C_3F_7BF_3^-$, $n-C_4F_9BF_3^-$, PF_6^-, $CF_3CO_2^-$, $CF_3SO_3^-$, $N(SO_2CF_3)_2^-$, $N(COCF_3)(SO_2CF_3)^-$, $N(SO_2F)_2^-$, $N(CN)_2^-$, $C(CN)_3^-$, SCN^-, $SeCN^-$, $CuCl_2^-$, $AlCl_4^-$, $F(HF)_{2.3}^-$, etc. Relatively speaking, the combination of imidazolium- or sulfonium-based cations and complex halide anions such as $AlCl_4^-$, BF_4^-, $CF_3CO_2^-$, $CF_3SO_3^-$, NTf_2^-, $N(SO_2F)_2^-$, or $F(HF)_{2.3}^-$ results in RTILs with good working conductivities.

RTILs can possess archetypical properties such as high intrinsic ionic conductivity, high thermal stability, low volatility, low (practically zero) vapor pressure, non-flammability, the ability to remain liquid at a wide range of temperatures above and below room temperature, high polarity, high viscosity, and wide electrochemical windows. These properties, except for the high viscosity, are desirable attributes when it comes to using an RTIL as an electrolyte ingredient (a salt and/or a solvent) in a supercapacitor.

In order to make a pseudo-capacitor (a supercapacitor that works on the development of pseudo-capacitance through redox pair formation), the anode active material or cathode active material may be designed to contain graphene sheets and a redox pair partner material selected from a metal oxide, a conducting polymer (e.g. conjugate-chain polymers), a non-conducting polymer (e.g. polyacrylonitrile, PAN), an organic material (e.g. hydroquinone), a non-graphene carbon material, an inorganic material, or a combination thereof. Many of the materials that can pair up with reduced graphene oxide sheets are well-known in the art. In this study, we have come to realize that graphene halogenide (e.g. graphene fluoride), graphene hydrogenide, and nitrogenated graphene can work with a wide variety of partner materials to form a redox pair for developing pseudo-capacitance.

For instance, the metal oxide or inorganic materials that serve in such a role include RuO_2, IrO_2, NiO, MnO_2, VO_2, V_2O_5, V_3O_8, TiO_2, Cr_2O_3, Co_2O_3, Co_3O_4, PbO_2, Ag_2O, MoC_x, Mo_2N, or a combination thereof. In general, the inorganic material may be selected from a metal carbide, metal nitride, metal boride, metal dichalcogenide, or a combination thereof. Preferably, the desired metal oxide or inorganic material is selected from an oxide, dichalcogenide, trichalcogenide, sulfide, selenide, or telluride of niobium, zirconium, molybdenum, hafnium, tantalum, tungsten, titanium, vanadium, chromium, cobalt, manganese, iron, or nickel in a nanowire, nano-disc, nano-ribbon, or nano platelet form. These materials or their precursors can be incorporated in the coating slurry prior to the coating or film forming procedure. Alternatively, their molecular precursors in a liquid solution may be impregnated into the pores of the

graphene foam and the precursor is then thermally or chemically converted into the desired inorganic species (e.g. transition metal oxide). The liquid or gel electrolyte is then impregnated into the foam.

The following examples are used to illustrate some specific details about the best modes of practicing the instant invention and should not be construed as limiting the scope of the invention.

Example 1

Various Blowing Agents and Pore-Forming (Bubble-Producing) Processes

In the field of plastic processing, chemical blowing agents are mixed into the plastic pellets in the form of powder or pellets and dissolved at higher temperatures. Above a certain temperature specific for blowing agent dissolution, a gaseous reaction product (usually nitrogen or CO_2) is generated, which acts as a blowing agent. However, a chemical blowing agent cannot be dissolved in a graphene material, which is a solid, not liquid. This presents a challenge to make use of a chemical blowing agent to generate pores or cells in a graphene material.

After extensive experimenting, we have discovered that practically any chemical blowing agent (e.g. in a powder or pellet form) can be used to create pores or bubbles in a dried layer of graphene when the first heat treatment temperature is sufficient to activate the blowing reaction. The chemical blowing agent (powder or pellets) may be dispersed in the liquid medium to become a second dispersed phase (sheets of graphene material being the first dispersed phase) in the suspension, which can be deposited onto the solid supporting substrate to form a wet layer. This wet layer of graphene material may then be dried and heat treated to activate the chemical blowing agent. After a chemical blowing agent is activated and bubbles are generated, the resulting foamed graphene structure is largely maintained even when subsequently a higher heat treatment temperature is applied to the structure. This is quite unexpected, indeed.

Chemical foaming agents (CFAs) can be organic or inorganic compounds that release gasses upon thermal decomposition. CFAs are typically used to obtain medium- to high-density foams, and are often used in conjunction with physical blowing agents to obtain low-density foams. CFAs can be categorized as either endothermic or exothermic, which refers to the type of decomposition they undergo. Endothermic types absorb energy and typically release carbon dioxide and moisture upon decomposition, while the exothermic types release energy and usually generate nitrogen when decomposed. The overall gas yield and pressure of gas released by exothermic foaming agents is often higher than that of endothermic types. Endothermic CFAs are generally known to decompose in the range of 130 to 230° C. (266-446° F.), while some of the more common exothermic foaming agents decompose around 200° C. (392° F.). However, the decomposition range of most exothermic CFAs can be reduced by addition of certain compounds. The activation (decomposition) temperatures of CFAs fall into the range of our heat treatment temperatures. Examples of suitable chemical blowing agents include sodium bicarbonate (baking soda), hydrazine, hydrazide, azodicarbonamide (exothermic chemical blowing agents), nitroso compounds (e.g. N, N-Dinitroso pentamethylene tetramine), hydrazine derivatives (e.g. 4. 4'-Oxybis (benzenesulfonyl hydrazide)

and Hydrazo dicarbonamide), and hydrogen carbonate (e.g. Sodium hydrogen carbonate). These are all commercially available in plastics industry.

In the production of foamed plastics, physical blowing agents are metered into the plastic melt during foam extrusion or injection molded foaming, or supplied to one of the precursor materials during polyurethane foaming. It has not been previously known that a physical blowing agent can be used to create pores in a graphene material, which is in a solid state (not melt). We have surprisingly observed that a physical blowing agent (e.g. CO_2 or N_2) can be injected into the stream of graphene suspension prior to being coated or cast onto the supporting substrate. This would result in a foamed structure even when the liquid medium (e.g. water and/or alcohol) is removed. The dried layer of graphene material is capable of maintaining a controlled amount of pores or bubbles during liquid removal and subsequent heat treatments.

Technically feasible blowing agents include Carbon dioxide (CO_2), Nitrogen (N_2), Isobutane (C_4H_{10}), Cyclopentane (C_5H_{10}), Isopentane (C_5H_{12}), CFC-11 ($CFCl_3$), HCFC-22 (CHF_2Cl), HCFC-142b (CF_2ClCH_3), and HCFC-134a (CH_2FCF_3). However, in selecting a blowing agent, environmental safety is a major factor to consider. The Montreal Protocol and its influence on consequential agreements pose a great challenge for the producers of foam. Despite the effective properties and easy handling of the formerly applied chlorofluorocarbons, there was a worldwide agreement to ban these because of their ozone depletion potential (ODP). Partially halogenated chlorofluorocarbons are also not environmentally safe and therefore already forbidden in many countries. The alternatives are hydrocarbons, such as isobutane and pentane, and the gases such as CO_2 and nitrogen.

Except for those regulated substances, all the blowing agents recited above have been tested in our experiments. For both physical blowing agents and chemical blowing agents, the blowing agent amount introduced into the suspension is defined as a blowing agent-to-graphene material weight ratio, which is typically from 0/1.0 to 1.0/1.0.

Example 2

Preparation of Discrete Nano Graphene Platelets (NGPs) which are GO Sheets

Chopped graphite fibers with an average diameter of 12 μm and natural graphite particles were separately used as a starting material, which was immersed in a mixture of concentrated sulfuric acid, nitric acid, and potassium permanganate (as the chemical intercalate and oxidizer) to prepare graphite intercalation compounds (GICs). The starting material was first dried in a vacuum oven for 24 h at 80° C. Then, a mixture of concentrated sulfuric acid, fuming nitric acid, and potassium permanganate (at a weight ratio of 4:1:0.05) was slowly added, under appropriate cooling and stirring, to a three-neck flask containing fiber segments. After 5-16 hours of reaction, the acid-treated graphite fibers or natural graphite particles were filtered and washed thoroughly with deionized water until the pH level of the solution reached 6. After being dried at 100° C. overnight, the resulting graphite intercalation compound (GIC) or graphite oxide fiber was re-dispersed in water and/or alcohol to form a slurry.

In one sample, five grams of the graphite oxide fibers were mixed with 2,000 ml alcohol solution consisting of alcohol and distilled water with a ratio of 15:85 to obtain a

slurry mass. Then, the mixture slurry was subjected to ultrasonic irradiation with a power of 200 W for various lengths of time. After 20 minutes of sonication, GO fibers were effectively exfoliated and separated into thin graphene oxide sheets with oxygen content of approximately 23%-31% by weight. The resulting suspension contains GO sheets being suspended in water. A chemical blowing agent (hydrazo dicarbonamide) was added to the suspension just prior to casting.

The resulting suspension was then cast onto a glass surface using a doctor's blade to exert shear stresses, inducing GO sheet orientations. The resulting GO coating films, after removal of liquid, have a thickness that can be varied from approximately 5 to 500 μm (preferably and typically from 10 μm to 50 μm).

For making a graphene foam specimen, the GO coating film was then subjected to heat treatments that typically involve an initial thermal reduction temperature of 80-350° C. for 1-8 hours, followed by heat-treating at a second temperature of 1,500-2,850° C. for 0.5 to 5 hours. It may be noted that we have found it essential to apply a compressive stress to the coating film sample while being subjected to the first heat treatment. This compress stress seems to have helped maintain good contacts between the graphene sheets so that chemical merging and linking between graphene sheets can occur while pores are being formed. Without such a compressive stress, the heat-treated film is typically excessively porous with constituent graphene sheets in the pore walls being very poorly oriented and incapable of chemical merging and linking with one another. As a result, the thermal conductivity, electrical conductivity, and mechanical strength of the graphene foam are severely compromised.

Example 3

Preparation of Single-Layer Graphene Sheets from Meso-Carbon Micro-Beads (MCMBs)

Meso-carbon microbeads (MCMBs) were supplied from China Steel Chemical Co., Kaohsiung, Taiwan. This material has a density of about 2.24 g/cm^3 with a median particle size of about 16 μm. MCMB (10 grams) were intercalated with an acid solution (sulfuric acid, nitric acid, and potassium permanganate at a ratio of 4:1:0.05) for 48-96 hours. Upon completion of the reaction, the mixture was poured into deionized water and filtered. The intercalated MCMBs were repeatedly washed in a 5% solution of HCl to remove most of the sulphate ions. The sample was then washed repeatedly with deionized water until the pH of the filtrate was no less than 4.5. The slurry was then subjected ultrasonication for 10-100 minutes to produce GO suspensions. TEM and atomic force microscopic studies indicate that most of the GO sheets were single-layer graphene when the oxidation treatment exceeded 72 hours, and 2- or 3-layer graphene when the oxidation time was from 48 to 72 hours. The GO sheets contain oxygen proportion of approximately 35%-47% by weight for oxidation treatment times of 48-96 hours. GO sheets were suspended in water. Baking soda (5-20% by weight), as a chemical blowing agent, was added to the suspension just prior to casting. The suspension was then cast onto a glass surface using a doctor's blade to exert shear stresses, inducing GO sheet orientations. Several samples were cast, some containing a blowing agent and some not. The resulting GO films, after removal of liquid, have a thickness that can be varied from approximately 10 to 500 μm.

The several sheets of the GO film, with or without a blowing agent, were then subjected to heat treatments that involve an initial (first) thermal reduction temperature of 80-500° C. for 1-5 hours. This first heat treatment generated a graphene foam. However, the graphene domains in the foam wall can be further perfected (re-graphitized to become more ordered or having a higher degree of crystallinity and larger lateral dimensions of graphene planes, longer than the original graphene sheet dimensions due to chemical merging) if the foam is followed by heat-treating at a second temperature of 1,500-2,850° C.

Example 4

Preparation of Pristine Graphene Foam (0% Oxygen)

Recognizing the possibility of the high defect population in GO sheets acting to reduce the conductivity of individual graphene plane, we decided to study if the use of pristine graphene sheets (non-oxidized and oxygen-free, non-halogenated and halogen-free, etc.) can lead to a graphene foam having a higher thermal conductivity. Pristine graphene sheets were produced by using the direct ultrasonication or liquid-phase production process.

In a typical procedure, five grams of graphite flakes, ground to approximately 20 μm or less in sizes, were dispersed in 1,000 mL of deionized water (containing 0.1% by weight of a dispersing agent, Zonyl® FSO from DuPont) to obtain a suspension. An ultrasonic energy level of 85 W (Branson S450 Ultrasonicator) was used for exfoliation, separation, and size reduction of graphene sheets for a period of 15 minutes to 2 hours. The resulting graphene sheets are pristine graphene that have never been oxidized and are oxygen-free and relatively defect-free. There are no other non-carbon elements.

Various amounts (1%-30% by weight relative to graphene material) of chemical bowing agents (N, N-Dinitroso pentamethylene tetramine or 4. 4'-Oxybis (benzenesulfonyl hydrazide) were added to a suspension containing pristine graphene sheets and a surfactant. The suspension was then cast onto a glass surface using a doctor's blade to exert shear stresses, inducing graphene sheet orientations. Several samples were cast, including one that was made using CO2 as a physical blowing agent introduced into the suspension just prior to casting). The resulting graphene films, after removal of liquid, have a thickness that can be varied from approximately 10 to 100 μm.

The graphene films were then subjected to heat treatments that involve an initial (first) thermal reduction temperature of 80-1,500° C. for 1-5 hours. This first heat treatment generated a graphene foam. Some of the pristine foam samples were then subjected to a second temperature of 1,500-2,850° C. to determine if the graphene domains in the foam wall could be further perfected (re-graphitized to become more ordered or having a higher degree of crystallinity).

Comparative Example 4

a: CVD Graphene Foams on Ni Foam Templates

The procedure was adapted from that disclosed in open literature: Chen, Z. et al. "Three-dimensional flexible and conductive interconnected graphene networks grown by chemical vapor deposition," Nat. Mater. 10, 424-428 (2011). Nickel foam, a porous structure with an interconnected 3D

scaffold of nickel was chosen as a template for the growth of graphene foam. Briefly, carbon was introduced into a nickel foam by decomposing CH_4 at 1,000° C. under ambient pressure, and graphene films were then deposited on the surface of the nickel foam. Due to the difference in the thermal expansion coefficients between nickel and graphene, ripples and wrinkles were formed on the graphene films. In order to recover (separate) graphene foam, Ni frame must be etched away. Before etching away the nickel skeleton by a hot HCl (or $FeCl_3$) solution, a thin layer of poly(methyl methacrylate) (PMMA) was deposited on the surface of the graphene films as a support to prevent the graphene network from collapsing during nickel etching. After the PMMA layer was carefully removed by hot acetone, a fragile graphene foam sample was obtained. The use of the PMMA support layer is critical to preparing a free-standing film of graphene foam; only a severely distorted and deformed graphene foam sample was obtained without the PMMA support layer. This is a tedious process that is not environmentally benign and is not scalable.

Comparative Example 4

b: Conventional Graphitic Foam from Pitch-Based Carbon Foams

Pitch powder, granules, or pellets are placed in a aluminum mold with the desired final shape of the foam. Mitsubishi ARA-24 meso-phase pitch was utilized. The sample is evacuated to less than 1 torr and then heated to a temperature approximately 300° C. At this point, the vacuum was released to a nitrogen blanket and then a pressure of up to 1,000 psi was applied. The temperature of the system was then raised to 800° C. This was performed at a rate of 2 degree C./min. The temperature was held for at least 15 minutes to achieve a soak and then the furnace power was turned off and cooled to room temperature at a rate of approximately 1.5 degree C./min with release of pressure at a rate of approximately 2 psi/min. Final foam temperatures were 630° C. and 800° C. During the cooling cycle, pressure is released gradually to atmospheric conditions. The foam was then heat treated to 1050° C. (carbonized) under a nitrogen blanket and then heat treated in separate runs in a graphite crucible to 2500° C. and 2800° C. (graphitized) in Argon.

Samples from the foam were machined into specimens for measuring the thermal conductivity. The bulk thermal conductivity ranged from 67 W/mK to 151 W/mK. The density of the samples was from 0.31-0.61 g/cm^3. When weight is taken into account, the specific thermal conductivity of the pitch derived foam is approximately 67/0.31=216 and 151/0.61=247.5 W/mK per specific gravity (or per physical density).

The compression strength of the samples having an average density of 0.51 g/cm^3 was measured to be 3.6 MPa and the compression modulus was measured to be 74 MPa. By contrast, the compression strength and compressive modulus of the presently invented graphene foam samples derived from GO having a comparable physical density are 5.7 MPa and 103 MPa, respectively.

Shown in FIG. 4(A) and FIG. 5(A) are the thermal conductivity values vs. specific gravity of the GO suspension-derived foam, meso-phase pitch-derived graphite foam, and Ni foam template-assisted CVD graphene foam. These data clearly demonstrate the following unexpected results:

1) GO-derived graphene foams produced by the presently invented process exhibit significantly higher thermal conductivity as compared to both meso-phase pitch-derived graphite foam and Ni foam template-assisted CVD graphene, given the same physical density.

2) This is quite surprising in view of the notion that CVD graphene is essentially pristine graphene that has never been exposed to oxidation and should have exhibited a much higher thermal conductivity compared to graphene oxide (GO). GO is known to be highly defective (having a high defect population and, hence, low conductivity) even after the oxygen-containing functional groups are removed via conventional thermal or chemical reduction methods. These exceptionally high thermal conductivity values observed with the GO-derived graphene foams herein produced are much to our surprise.

3) FIG. 5(A) presents the thermal conductivity values over comparable ranges of specific gravity values to allow for calculation of specific conductivity (conductivity value, W/mK, divided by physical density value, g/cm^3) for all three graphitic foam materials based on the slopes of the curves (approximately straight lines at different segments). These specific conductivity values enable a fair comparison of thermal conductivity values of these three types of graphitic foams given the same amount of solid graphitic material in each foam. These data provide an index of the intrinsic conductivity of the solid portion of the foam material. These data clearly indicate that, given the same amount of solid material, the presently invented GO-derived foam is intrinsically most conducting, reflecting a high level of graphitic crystal perfection (larger crystal dimensions, fewer grain boundaries and other defects, better crystal orientation, etc.). This is also unexpected.

4) The specific conductivity values of the presently invented GO- and GF-derived foam exhibit values from 250 to 500 W/mK per unit of specific gravity; but those of the other two foam materials are typically lower than 250 W/mK per unit of specific gravity.

Summarized in FIG. 7 are thermal conductivity data for a series of GO-derived graphene foams and a series of pristine graphene derived foams, both plotted over the final (maximum) heat treatment temperatures. These data indicate that the thermal conductivity of the GO foams is highly sensitive to the final heat treatment temperature (HTT). Even when the HTT is very low, clearly some type of graphene merging or crystal perfection reactions are already activated. The thermal conductivity increases monotonically with the final HTT. In contrast, the thermal conductivity of pristine graphene foams remains relatively constant until a final HTT of approximately 2,500° C. is reached, signaling the beginning of a re-crystallization and perfection of graphite crystals. There are no functional groups in pristine graphene, such as —COOH in GO, that enable chemical linking of graphene sheets at relatively low HTTs. With a HTT as low as 1,250° C., GO sheets can merge to form significantly larger graphene sheets with reduced grain boundaries and other defects. Even though GO sheets are intrinsically more defective than pristine graphene, the presently invented process enables the GO sheets to form graphene foams that outperform pristine graphene foams. This is another unexpected result.

Example 5

Preparation of Graphene Oxide (GO) Suspension from Natural Graphite and of Subsequent GO Foams

Graphite oxide was prepared by oxidation of graphite flakes with an oxidizer liquid consisting of sulfuric acid,

sodium nitrate, and potassium permanganate at a ratio of 4:1:0.05 at 30° C. When natural graphite flakes (particle sizes of 14 μm) were immersed and dispersed in the oxidizer mixture liquid for 48 hours, the suspension or slurry appears and remains optically opaque and dark. After 48 hours, the reacting mass was rinsed with water 3 times to adjust the pH value to at least 3.0. A final amount of water was then added to prepare a series of GO-water suspensions. We observed that GO sheets form a liquid crystal phase when GO sheets occupy a weight fraction >3% and typically from 5% to 15%.

By dispensing and coating the GO suspension on a polyethylene terephthalate (PET) film in a slurry coater and removing the liquid medium from the coated film we obtained a thin film of dried graphene oxide. Several GO film samples were then subjected to different heat treatments, which typically include a thermal reduction treatment at a first temperature of 100° C. to 500° C. for 1-10 hours, and at a second temperature of 1,500° C.-2,850° C. for 0.5-5 hours. With these heat treatments, also under a compressive stress, the GO films were transformed into graphene foam.

Comparative Example 5

a: Graphene Foams from Hydrothermally Reduced Graphene Oxide

For comparison, a self-assembled graphene hydrogel (SGH) sample was prepared by a one-step hydrothermal method. In a typical procedure, the SGH can be easily prepared by heating 2 mg/mL of homogeneous graphene oxide (GO) aqueous dispersion sealed in a Teflon-lined autoclave at 180° C. for 12 h. The SGH containing about 2.6% (by weight) graphene sheets and 97.4% water has an electrical conductivity of approximately 5×10^{-3} S/cm. Upon drying and heat treating at 1,500° C., the resulting graphene foam exhibits an electrical conductivity of approximately 1.5×10^{-1} S/cm, which is 2 times lower than those of the presently invented graphene foams produced by heat treating at the same temperature.

Comparative Example 5

b: Plastic Bead Template-Assisted Formation of Reduced Graphene Oxide Foams

A hard template-directed ordered assembly for a macro-porous bubbled graphene film (MGF) was prepared. Mono-disperse poly methyl methacrylate (PMMA) latex spheres were used as the hard templates. The GO liquid crystal prepared in Example 5 was mixed with a PMMA spheres suspension. Subsequent vacuum filtration was then conducted to prepare the assembly of PMMA spheres and GO sheets, with GO sheets wrapped around the PMMA beads. A composite film was peeled off from the filter, air dried and calcinated at 800° C. to remove the PMMA template and thermally reduce GO into RGO simultaneously. The grey free-standing PMMA/GO film turned black after calcination, while the graphene film remained porous.

FIG. 4(B) and FIG. 5(B) show the thermal conductivity values of the presently invented GO suspension-derived foam, GO foam produced via sacrificial plastic bead template-assisted process, and hydrothermally reduced GO graphene foam. Most surprisingly, given the same starting GO sheets, the presently invented process produces the highest-performing graphene foams. Electrical conductivity data summarized in FIG. 4(C) are also consistent with this

conclusion. These data further support the notion that, given the same amount of solid material, the presently invented GO suspension deposition (with stress-induced orientation) and subsequent heat treatments give rise to a graphene foam that is intrinsically most conducting, reflecting a highest level of graphitic crystal perfection (larger crystal dimensions, fewer grain boundaries and other defects, better crystal orientation, etc. along the pore walls).

It is of significance to point out that all the prior art processes for producing graphite foams or graphene foams appear to provide macro-porous foams having a physical density in the range of approximately 0.2-0.6 g/cm³ only with pore sizes being typically too large (e.g. from 20 to 300 μm) for most of the intended applications. In contrast, the instant invention provides processes that generate graphene foams having a density that can be as low as 0.01 g/cm³ and as high as 1.7 g/cm³. The pore sizes can be varied between meso-scaled (2-50 nm) up to macro-scaled (1-500 μm) depending upon the contents of non-carbon elements and the amount/type of blowing agent used. This level of flexibility and versatility in designing various types of graphene foams is unprecedented and un-matched by any prior art process.

Example 6

Preparation of Graphene Foams from Graphene Fluoride

Several processes have been used by us to produce GF, but only one process is herein described as an example. In a typical procedure, highly exfoliated graphite (HEG) was prepared from intercalated compound $C_2F \cdot xClF_3$. HEG was further fluorinated by vapors of chlorine trifluoride to yield fluorinated highly exfoliated graphite (FHEG). Pre-cooled Teflon reactor was filled with 20-30 mL of liquid pre-cooled ClF_3, the reactor was closed and cooled to liquid nitrogen temperature. Then, no more than 1 g of HEG was put in a container with holes for ClF_3 gas to access and situated inside the reactor. In 7-10 days a gray-beige product with approximate formula C_2F was formed.

Subsequently, a small amount of FHEG (approximately 0.5 mg) was mixed with 20-30 mL of an organic solvent (methanol, ethanol, 1-propanol, 2-propanol, 1-butanol, tert-butanol, isoamyl alcohol) and subjected to an ultrasound treatment (280 W) for 30 min, leading to the formation of homogeneous yellowish dispersions. Five minutes of sonication was enough to obtain a relatively homogenous dispersion, but longer sonication times ensured better stability. Upon casting on a glass surface with the solvent removed, the dispersion became a brownish film formed on the glass surface. When GF films were heat-treated, fluorine was released as gases that helped to generate pores in the film. In some samples, a physical blowing agent (N_2 gas) was injected into the wet GF film while being cast. These samples exhibit much higher pore volumes or lower foam densities. Without using a blowing agent, the resulting graphene fluoride foams exhibit physical densities from 0.35 to 1.38 g/cm³. When a blowing agent was used (blowing agent/GF weight ratio from 0.5/1 to 0.05/1), a density from 0.02 to 0.35 g/cm³ was obtained. Typical fluorine contents are from 0.001% (HTT=2,500° C.) to 4.7% (HTT=350° C.), depending upon the final heat treatment temperature involved.

FIG. 6 presents a comparison in thermal conductivity values of the graphene foam samples derived from GO and GF (graphene fluoride), respectively, as a function of the specific gravity. It appears that the GF foams, in comparison with GO foams, exhibit higher thermal conductivity values at comparable specific gravity values. Both deliver impressive heat-conducting capabilities, being the best among all known foamed materials.

Example 7

Preparation of Graphene Foams from Nitrogenataed Graphene

Graphene oxide (GO), synthesized in Example 2, was finely ground with different proportions of urea and the pelletized mixture heated in a microwave reactor (900 W) for 30 s. The product was washed several times with deionized water and vacuum dried. In this method graphene oxide gets simultaneously reduced and doped with nitrogen. The products obtained with graphene:urea mass ratios of 1:0.5, 1:1 and 1:2 are designated as NGO-1, NGO-2 and NGO-3 respectively and the nitrogen contents of these samples were 14.7, 18.2 and 17.5 wt % respectively as found by elemental analysis. These nitrogenataed graphene sheets remain dispersible in water. The resulting suspensions were then cast, dried, and heat-treated initially at 200-350° C. as a first heat treatment temperature and subsequently treated at a second temperature of 1,500° C. The resulting nitrogenated graphene foams exhibit physical densities from 0.45 to 1.28 g/cm^3. Typical nitrogen contents of the foams are from 0.01% (HTT=1,500° C.) to 5.3% (HTT=350° C.), depending upon the final heat treatment temperature involved.

Example 8

Characterization of Various Graphene Foams and Conventional Graphite Foam

The internal structures (crystal structure and orientation) of several dried GO layers, and the heat-treated films at different stages of heat treatments were investigated using X-ray diffraction. The X-ray diffraction curve of natural graphite typically exhibits a peak at approximately $2\theta=26°$, corresponds to an inter-graphene spacing (d_{002}) of approximately 0.3345 nm. Upon oxidation, the resulting GO shows an X-ray diffraction peak at approximately $2\theta=12°$, which corresponds to an inter-graphene spacing (d_{002}) of approximately 0.7 nm. With some heat treatment at 150° C., the dried GO compact exhibits the formation of a hump centered at 22°, indicating that it has begun the process of decreasing the inter-graphene spacing due to the beginning of chemical linking and ordering processes. With a heat treatment temperature of 2,500° C. for one hour, the d_{002} spacing has decreased to approximately 0.336, close to 0.3354 nm of a graphite single crystal.

With a heat treatment temperature of 2,750° C. for one hour, the d_{002} spacing is decreased to approximately to 0.3354 nm, identical to that of a graphite single crystal. In addition, a second diffraction peak with a high intensity appears at $2\theta=55°$ corresponding to X-ray diffraction from (004) plane. The (004) peak intensity relative to the (002) intensity on the same diffraction curve, or the I(004)/I(002) ratio, is a good indication of the degree of crystal perfection and preferred orientation of graphene planes. The (004) peak is either non-existing or relatively weak, with the I(004)/I (002) ratio <0.1, for all graphitic materials heat treated at a temperature lower than 2,800° C. The I(004)/I(002) ratio for

the graphitic materials heat treated at 3,000-3,250° C. (e,g, highly oriented pyrolytic graphite, HOPG) is in the range of 0.2-0.5. In contrast, a graphene foam prepared with a final HTT of 2,750° C. for one hour exhibits a I(004)/I(002) ratio of 0.78 and a Mosaic spread value of 0.21, indicating a practically perfect graphene single crystal with a good degree of preferred orientation.

The "mosaic spread" value is obtained from the full width at half maximum of the (002) reflection in an X-ray diffraction intensity curve. This index for the degree of ordering characterizes the graphite or graphene crystal size (or grain size), amounts of grain boundaries and other defects, and the degree of preferred grain orientation. A nearly perfect single crystal of graphite is characterized by having a mosaic spread value of 0.2-0.4. Some of our graphene foams have a mosaic spread value in this range of 0.2-0.4 when produced using a final heat treatment temperature no less than 2,500° C.

The inter-graphene spacing values of both the GO suspension-derived samples obtained by heat treating at various temperatures over a wide temperature range are summarized in FIG. 8(A). Corresponding oxygen content values in the GO suspension-derived unitary graphene layer are shown in FIG. 8(B).

It is of significance to point out that a heat treatment temperature as low as 500° C. is sufficient to bring the average inter-graphene spacing in GO sheets along the pore walls to below 0.4 nm, getting closer and closer to that of natural graphite or that of a graphite single crystal. The beauty of this approach is the notion that this GO suspension strategy has enabled us to re-organize, re-orient, and chemically merge the planar graphene oxide molecules from originally different graphite particles or graphene sheets into a unified structure with all the graphene planes now being larger in lateral dimensions (significantly larger than the length and width of the graphene planes in the original graphite particles). A potential chemical linking mechanism is illustrated in FIG. 3. This has given rise to exceptional thermal conductivity and electrical conductivity values.

Example 9

Preparation of Intrinsically Conductive Polymer—Graphene Redox Pairs in a Graphene

In this series of examples, intrinsically conductive polymers (e.g. polyaniline, poly polypyrrole, and polythiophene) and their sulfonated versions are evaluated for their effectiveness as a redox pair partner material with a graphene material.

The chemical synthesis of the sulfonated polyaniline (S-PANi) was accomplished by reacting polyaniline with concentrated sulfuric acid. The procedure was similar to that used by Epstein, et al. (U.S. Pat. No. 5,109,070, Apr. 28, 1992). The resulting S-PANi can be represented by the following Formula 1, with R_1, R_2, R_3, and R_4 group being H, SO_3^- or SO_3H (R_5=H) with the content of the latter two being varied between 30% and 75% (i.e., the degree of sulfonation varied between 30% and 75%).
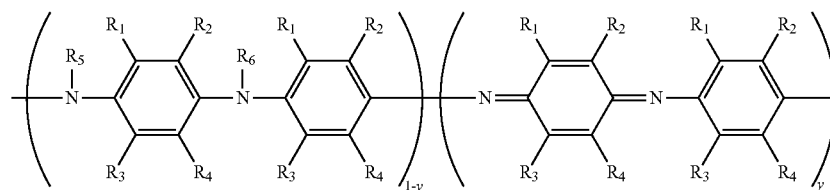
(Formula 1)

The electron conductivity of these SO_3^- or SO_3H-based S-PANi compositions in the range of 0.1 S/cm to 0.5 S/cm when the degree of sulfonation was from approximately 30% to 75% (with y being approximately 0.4-0.6). The S-PANi/water solution was impregnated into a solid graphene foam and, upon water removal, the S-PANi is precipitated out and coated onto the graphene-based pore walls for forming a redox or pseudo-capacitance electrode. Non-sulfonated polymers can be dissolved in select organic solvents.

A sulfonated pyrrole-based polymer (with X=NH and Y=SO_3^-, m=1, and A=H in the following formula) was synthesized by following a procedure adapted from Aldissi, et al., U.S. Pat. No. 4,880,508, Nov. 14, 1989.

(Formula 2)

$$\begin{array}{c} X \\ -C \diagup \diagdown C- \\ \parallel \quad \parallel \\ H-C \text{———} C-(CH_2)_m-Y-A \end{array}$$
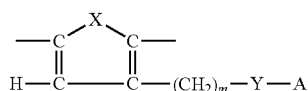
For solution impregnation, as one example, approximately 5.78 g of the resulting sulfonated polypyrrole was dissolved in 100 ml of distilled water. Then, the aqueous solution was impregnated into pores of a graphene foam and dried to allow for precipitation and deposition of sulfonated polypyrrole onto surfaces of graphene-based pore walls to form a redox pair with graphene in the pore walls.

Water-soluble conductive polymers having a thiophene ring (X=sulfur) and alkyl groups containing 4 carbon atoms (m=4) in the above Formula 2 were prepared, according to a method adapted from Aldissi, et al. (U.S. Pat. No. 4,880, 508, Nov. 14, 1989). The surfactant molecules of these polymers were sulfonate groups with sodium. Conductivity of this polymer in a self-doped state was found to be from about 10^{-3} to about 10^{-2} S/cm. When negative ions from a supporting electrolyte used during synthesis were allowed to remain in the polymer, conductivities up to about 50 S/cm were observed.

A doped poly (alkyl thiophene) (PAT) with Y=SO_3H and A=H in Formula 2 that exhibited an electron conductivity of 12.5 S/cm was dissolved in an aqueous hydrogen peroxide (H_2O_2) solution. The resulting polymer solution was impregnated into a solid graphene foam and dried to form a redox or pseudo-capacitance electrode.

We have surprisingly discovered that the sulfonated version (e.g. S-PANi) of an intrinsically conductive polymer (PANi), when paired up with a graphene foam material, leads to a significantly higher pseudo-capacitance value when compared with the un-sulfonated one; e.g. 654 F/g (S-PANi) vs. 463 F/g (PANi) and 487 F/cm³ (S-PPy) vs. 355 F/cm³ (PPy).

Example 10

Preparation of MnO_2—Graphene Redox Pairs in a Graphene Foam

The MnO_2 powder was synthesized by two methods (one with the presence of pristine graphene and the other within the pores of graphene-carbon foam). In one method, a 0.1 mol/L $KMnO_4$ aqueous solution was prepared by dissolving potassium permanganate in deionized water. Meanwhile 13.3 g surfactant of high purity sodium bis(2-ethylhexyl) sulfosuccinate was added in 300 mL iso-octane (oil) and stirred well to obtain an optically transparent solution. Then,

32.4 mL of 0.1 mol/L $KMnO_4$ solution were added in the solution, and a piece of graphene-carbon hybrid foam was immersed in the solution. On a separate basis, pristine graphene sheets were added into the solution. The two pots of resulting suspensions were ultrasonicated for 30 min and a dark brown precipitate of MnO_2 was coated on surfaces of the foam walls and graphene sheets, respectively. The products were recovered, washed several times with distilled water and ethanol, and dried at 80° C. for 12 h. The samples were (1) a graphene-carbon hybrid foam structure having graphene wall-supported MnO_2 and (2) MnO_2-coated graphene sheets, which were then packed into a porous paper-like structure using the vacuum-assisted filtration method. In both cases, graphene and MnO_2 form a redox pair operating to produce pseudo-capacitance when a liquid electrolyte is impregnated into pores of the foam. With comparable electrode thickness (approximately 105 μm), the graphene foam-based electrode exhibits a significantly lower equivalent series resistance.

Example 11

Evaluation of Various Supercapacitor Cells

In most of the examples investigated, both the inventive supercapacitor cells and their conventional counterparts were fabricated and evaluated. The latter cells, for comparison purposes, were prepared by the conventional procedures of slurry coating of electrodes, drying of electrodes, assembling of anode layer, separator, and cathode layer, packaging of assembled laminate, and injection of liquid electrolyte. In a conventional cell, an electrode (cathode or anode), is typically composed of 85% an electrode active material (e.g. graphene, activated carbon, inorganic nano discs, etc.), 5% Super-P (acetylene black-based conductive additive), and 10% PTFE, which were mixed and coated on Al foil. The thickness of electrode is around 100 μm. For each sample, both coin-size and pouch cells were assembled in a glove box. The capacity was measured with galvanostatic experiments using an Arbin SCTS electrochemical testing instrument. Cyclic voltammetry (CV) and electrochemical impedance spectroscopy (EIS) were conducted on an electrochemical workstation (CHI 660 System, USA).

Galvanostatic charge/discharge tests were conducted on the samples to evaluate the electrochemical performance. For the galvanostatic tests, the specific capacity (q) is calculated as

$$q=I^*t/m \tag{1}$$

where I is the constant current in mA, t is the time in hours, and m is the cathode active material mass in grams. With voltage V, the specific energy (E) is calculated as,

$$E=\int Vdq \tag{2}$$

The specific power (P) can be calculated as

$$P=(E/t)(W/kg) \tag{3}$$

where t is the total charge or discharge step time in hours.

The specific capacitance (C) of the cell is represented by the slope at each point of the voltage vs. specific capacity plot,

$$C=dq/dV \tag{4}$$

For each sample, several current density (representing charge/discharge rates) were imposed to determine the electrochemical responses, allowing for calculations of energy

density and power density values required of the construction of a Ragone plot (power density vs. energy density).

Example 12

Achievable Electrode Tap Density and its Effect on Electrochemical Performance of Supercapacitor Cells

The presently invented process allows us to prepare graphene foam of any practical tap density from 0.1 to 1.3 g/cm³. Tap densities higher than 1.3 g/cm³ are possible, but the spaces between graphene sheets become too limited to accommodate a sufficient amount of electrolyte. It may be noted that the graphene-based supercapacitor electrodes prepared by conventional processes are limited to <0.3 and mostly <0.2 g/cm³. Furthermore, as discussed earlier, only thinner electrodes can be prepared using these conventional processes. As a point of reference, the activated carbon-based electrode exhibits a tap density typically from 0.3 to 0.5 g/cm³.

A series of EDLC electrodes with varying tap densities were prepared from the same batch of graphene foam sheet, but roll-pressed to different extents. The volume and weights of an electrode were measured before and after electrolyte impregnation and before and after roll-pressing. These measurements enabled us to estimate the tap density of the dried electrode (wet electrode volume/weight minus the amount of electrolyte actually absorbed). For comparison purposes, graphene-based electrodes of comparable thickness (70-75 μm) were also prepared using the conventional slurry coating process (the wet-dry-wet procedures). The electrode specific capacitance values of these supercapacitors using an organic electrolyte (acetonitrile) are summarized in FIG. 9. There are several significant observations that can be made from these data:

  (A) Given comparable electrode thickness, the presently invented graphene foam electrodes exhibit significantly higher gravimetric specific capacitance (185-289 F/g) as compared to those (131-145 F/g) of the corresponding graphene-based electrodes prepared by the conventional process, all based on EDLC alone.

  (B) The highest achievable tap density of the electrode prepared by the conventional method is 0.14-0.28 g/cm³. In contrast, the presently invented process makes it possible to achieve a tap density of 0.35-1.61 g/cm³; these unprecedented values even surpass those (0.3-0.5 g/cm³) of activated carbon electrodes by a large margin.

  (C) The presently invented graphene foam electrodes exhibit a volumetric specific capacitance up to 338 F/cm³, which is also an unprecedented value. In contrast, the graphene electrodes prepared according to the conventional method shows a specific capacitance in the range of 20-37 F/cm³; the differences are dramatic.

Shown in FIG. 10 are Ragone plots (gravimetric and volumetric power density vs. energy density) of two sets of symmetric supercapacitor (EDLC) cells containing nitrogen-doped graphene sheets and nitrogen-doped graphene foam as the electrode active material and EMIMBF4 ionic liquid as the electrolyte. One of the two series of supercapacitors was based on the graphene foam electrode prepared according to an embodiment of instant invention and the other was by the conventional slurry coating of electrodes. Several significant observations can be made from these data:

  (A) Both the gravimetric and volumetric energy densities and power densities of the supercapacitor cells prepared by the presently invented method (denoted as "inventive" in the figure legend) are significantly higher than those of their counterparts prepared via the conventional method (denoted as "conventional"). The differences are highly dramatic and are mainly due to the high active material mass loading (>20 mg/cm²) associated with the presently invented cells, reduced proportion of overhead components (non-active) relative to the active material weight/volume, no binder resin, the ability of the inventive method to more effectively pack graphene sheets together without graphene sheet re-stacking (pre-impregnated electrolyte serving as a spacer).

  (B) For the cells prepared by the conventional method, the absolute magnitudes of the volumetric energy densities and volumetric power densities are significantly lower than those of their gravimetric energy densities and gravimetric power densities, due to the very low tap density (packing density of 0.28 g/cm³) of isolated graphene sheet-based electrodes prepared by the conventional slurry coating method.

  (C) In contrast, for the cells prepared by the presently invented method, the absolute magnitudes of the volumetric energy densities and volumetric power densities are higher than those of their gravimetric energy densities and gravimetric power densities, due to the relatively high tap density (packing density of 1.2 g/cm³) of graphene foam-based electrodes prepared by the presently invented method.

Shown in FIG. 11 are Ragone plots of lithium ion capacitor (LIC) cells containing pristine graphene sheets as the cathode active material, prelithiated graphite particles as the anode active material, and lithium salt (LiPF₆)-PC/DEC as organic liquid electrolyte. The data are for both LICs, wherein the cathode is prepared by the presently invented electrolyte-impregnated graphene foam method and those by the conventional slurry coating of electrodes. These data indicate that both the gravimetric and volumetric energy densities and power densities of the LIC cells prepared by the presently invented method are significantly higher than those of their counterparts prepared via the conventional method. Again, the differences are huge and are mainly ascribed to the high active material mass loading (>25 mg/cm² at the cathode side) associated with the presently invented cells, reduced proportion of overhead (non-active) components relative to the active material weight/volume, no binder resin, the ability of the inventive method to more effectively pack graphene sheets together without re-stacking.

For the LIC cells prepared by the conventional method, the absolute magnitudes of the volumetric energy densities and volumetric power densities are significantly lower than those of their gravimetric energy densities and gravimetric power densities, due to the very low tap density (packing density of 0.28 g/cm³) of pristine graphene-based cathodes prepared by the conventional slurry coating method. In contrast, for the LIC cells prepared by the instant method, the absolute magnitudes of the volumetric energy densities and volumetric power densities are higher than those of their gravimetric energy densities and gravimetric power densities, due to the relatively high tap density of pristine graphene-based cathodes prepared by the presently invented method.

It is of significance to point out that reporting the energy and power densities per weight of active material alone on

a Ragone plot, as did by many researchers, may not give a realistic picture of the performance of the assembled super-capacitor cell. The weights of other device components also must be taken into account. These overhead components, including current collectors, electrolyte, separator, binder, connectors, and packaging, are non-active materials and do not contribute to the charge storage amounts. They only add weights and volumes to the device. Hence, it is desirable to reduce the relative proportion of overhead component weights and increase the active material proportion. How-ever, it has not been possible to achieve this objective using conventional supercapacitor production processes. The pres-ent invention overcomes this long-standing, most serious problem in the art of supercapacitors.

In a commercial supercapacitor having an electrode thick-ness of 150 μm, the weight of the active material (i.e. activated carbon) accounts for about 30% of the total mass of the packaged cell. Hence, a factor of 3 to 4 is frequently used to extrapolate the energy or power densities of the device (cell) from the properties based on the active material weight alone. In most of the scientific papers, the properties reported are typically based on the active material weight alone and the electrodes are typically very thin (<<100 μm, and mostly <<50 μm). The active material weight is typi-cally from 5% to 10% of the total device weight, which implies that the actual cell (device) energy or power densi-ties may be obtained by dividing the corresponding active material weight-based values by a factor of 10 to 20. After this factor is taken into account, the properties reported in these papers do not really look any better than those of commercial supercapacitors. Thus, one must be very careful when it comes to read and interpret the performance data of supercapacitors reported in the scientific papers and patent applications.

Example 13

Achievable Electrode Thickness and its Effect on Electrochemical Performance of Supercapacitor Cells

One might be tempted to think the electrode thickness of a supercapacitor is a design parameter that can be freely adjusted for optimization of device performance; but, in reality, the supercapacitor thickness is manufacturing-lim-ited and one cannot produce electrodes of good structural integrity that exceed certain thickness level. Our studies further indicate that this problem is even more severe with graphene-based electrode. The instant invention solves this critically important issue associated with supercapacitors.

The presently invented process allows us to prepare graphene foam of any thickness from 10 nm to 10 mm (or even thicker). However, for practical purposes, we typically prepare graphene foam sheets from 5 μm to 500 μm thick. When thicker electrodes are desired, we can stack multiple sheets of electrolyte-impregnated foam to reach essentially any reasonable electrode thickness. By contrast, the conven-tional wet-dry-wet process does not allow for such flexibil-ity.

Also highly significant and unexpected are the data sum-marized in FIG. **12** for reduced graphene oxide-based EDLC supercapacitors. The cell-level gravimetric and volumetric energy densities plotted over the achievable electrode thick-ness range of the RGO-based EDLC supercapacitors (or-ganic liquid electrolyte) prepared via the conventional method and those by the presently invented method (oxi-dized graphene foam). In this figure, the gravimetric (♦) and

volumetric (▲) energy density of the conventional superca-paitors are based on the highest achieved electrode tap density of approximately 0.28 g/cm³, and the gravimetric (■) and volumetric (x) energy density of the presently invented supercapaitors are from those having an electrode tap density of approximately 0.95 g/cm³, by no means the highest. No one else has previously reported such a high tap density for un-treated, non-activated oxidized graphene electrodes.

These data indicate that the highest gravimetric energy density achieved with RGO-based EDLC supercapacitor cells produced by the conventional slurry coating method is approximately 15.8 Wh/kg, but those prepared by the pres-ently invented method exhibit a gravimetric energy density as high as 43.9 Wh/kg at room temperature. This is an unprecedentedly high energy density value for EDLC super-capacitors (based on the total cell weight, not the electrode weight or active material weight alone). Even more impres-sive is the observation that the volumetric energy density of the presently invented supercapacitor cell is as high as 54.9 Wh/L, which is more than 10 times greater than the 4.4 Wh/L achieved by the conventional counterparts.

Example 14

Achievable Active Material Weight Percentage in a Cell and its Effect on Electrochemical Performance of Supercapacitor Cells

Because the active material weight accounts for up to about 30% of the total mass of the packaged commercial supercapacitors, a factor of 30% must be used to extrapolate the energy or power densities of the device from the per-formance data of the active material alone. Thus, the energy density of 20 Wh/kg of activated carbon (i.e. based on the active material weight alone) will translate to about 6 Wh/kg of the packaged cell. However, this extrapolation is only valid for electrodes with thicknesses and densities similar to those of commercial electrodes (150 μm or about 10 mg/cm² of the carbon electrode). An electrode of the same active material that is thinner or lighter will mean an even lower energy or power density based on the cell weight. Thus, it would be desirable to produce a supercapacitor cell having a high active material proportion. Unfortunately, it has not been previously possible to achieve an active material proportion greater than 30% by weight for activated carbon-based supercapacitors or greater than 15% by weight for graphene-based supercapacitors.

The presently invented method enables the supercapaci-tors to go well beyond these limits for all active materials investigated. As a matter of fact, the instant invention makes it possible to elevate the active material proportion above 90% if so desired; but typically from 15% to 85%, more typically from 30% to 80%, even more typically from 40% to 75%, and most typically from 50% to 70%. For instance, FIG. **13** shows the cell-level gravimetric energy densities plotted over the achievable active material proportion (ac-tive material weight/total cell weight) in a graphene-carbon hybrid foam-based EDLC supercapacitor (with organic liq-uid electrolyte). An exceptional cell-level energy density of 46.6 Wh/kg has been achieved.

In conclusion, we have successfully developed an abso-lutely new, novel, unexpected, and patently distinct class of highly conducting graphene foam materials and related processes of production. These foam materials prove to be exceptional supercapacitor electrode active materials. The chemical composition (% of oxygen, fluorine, and other

non-carbon elements), structure (crystal perfection, grain size, defect population, etc), crystal orientation, morphology, process of production, and properties of this new class of foam materials are fundamentally different and patently distinct from meso-phase pitch-derived, graphite foam, CVD graphene-derived foam, and graphene foams from hydrothermal reduction of GO, and sacrificial bead template-assisted RGO foam. The thermal conductivity, electrical conductivity, elastic modulus, and flexural strength exhibited by the presently invented foam materials are much higher than what prior art foam materials.

We claim:

1. A process for producing a supercapacitor electrode, said process comprising:

(a) preparing a graphene dispersion having multiple sheets of a starting graphene material dispersed in a liquid medium, and wherein said dispersion contains an optional blowing agent having a blowing agent-to-graphene material weight ratio from 0/1.0 to 1.0/1.0;

(b) dispensing and depositing said graphene dispersion onto a surface of a supporting substrate to form a wet layer of graphene material, wherein said dispensing and depositing procedure includes subjecting said graphene dispersion to an orientation-inducing stress;

(c) partially or completely removing said liquid medium from the wet layer of graphene material to form a dried layer of graphene material;

(d) heat treating the dried layer of graphene material at a first heat treatment temperature from 80° C. to 3,200° C. at a desired heating rate sufficient to induce volatile gas molecules from said non-carbon elements or to activate said blowing agent for producing a layer of solid graphene foam, wherein said solid graphene foam is composed of multiple pores and pore walls, and said pore walls contain a pristine graphene material having essentially zero % of non-carbon elements, or a non-pristine graphene material having 0.001% to 5% by weight of non-carbon elements, and wherein said solid graphene foam has a physical density from 0.01 to 1.7 g/cm^3, a specific surface area from 50 to 3,300 m^2/g, a thermal conductivity of at least 200 W/mK per unit of specific gravity, and/or an electrical conductivity no less than 2,000 S/cm per unit of specific gravity; and

(e) impregnating said multiple pores with a liquid or gel electrolyte to form a layer of pre-impregnated solid graphene foam, which is subjected to a step of compressing or roll-pressing that reduces a pore size, improves orientation of graphene planes, and squeezes excess electrolyte out of said pre-impregnated solid graphene foam for forming said supercapacitor electrode.

2. The process of claim 1, wherein said starting graphene material is selected from a pristine graphene or a non-pristine graphene material, having a content of non-carbon elements greater than 2% by weight, selected from graphene oxide, reduced graphene oxide, graphene fluoride, graphene chloride, graphene bromide, graphene iodide, hydrogenated graphene, nitrogenated graphene, chemically functionalized graphene, doped graphene, or a combination thereof.

3. The process of claim 1, further including a step of heat-treating the solid graphene foam at a second heat treatment temperature higher than said first heat treatment temperature, prior to step (e), for a length of time sufficient for obtaining a graphene foam wherein said pore walls contain stacked graphene planes having an inter-plane spacing d_{002} from 0.3354 nm to 0.36 nm and a content of non-carbon elements less than 2% by weight.

4. The process of claim 1, wherein said graphene material contains pristine graphene and said dispersion contains a blowing agent having a blowing agent-to-pristine graphene weight ratio from 0.01/1.0 to 1.0/1.0.

5. The process of claim 1, wherein said blowing agent is a physical blowing agent, a chemical blowing agent, a mixture thereof, a dissolution-and-leaching agent, or a mechanically introduced blowing agent.

6. The process of claim 1, wherein said graphene material is selected from the group of non-pristine graphene materials consisting of graphene oxide, reduced graphene oxide, graphene fluoride, graphene chloride, graphene bromide, graphene iodide, hydrogenated graphene, nitrogenated graphene, chemically functionalized graphene, doped graphene, and combinations thereof, and wherein the first heat treatment temperature is less than 2,500° C. and said solid graphene foam contains a content of non-carbon elements from 0.01% to 2.0% by weight.

7. The process of claim 3, wherein said graphene material is selected from the group of non-pristine graphene materials consisting of graphene oxide, reduced graphene oxide, graphene fluoride, graphene chloride, graphene bromide, graphene iodide, hydrogenated graphene, nitrogenated graphene, chemically functionalized graphene, doped graphene, and combinations thereof, and wherein both the first and second heat treatment temperatures are less than 2,500° C. and said solid graphene foam contains a content of non-carbon elements in the range of 0.01% to 2.0% by weight.

8. The process of claim 1, wherein said graphene material in said solid graphene foam contains structural defects induced during said step (d) of heat treating.

9. The process of claim 1, wherein said liquid medium consists of water and/or an alcohol.

10. The process of claim 1, which is a roll-to-roll process wherein said steps (b) and (c) include feeding said supporting substrate from a feeder roller to a deposition zone, continuously or intermittently depositing said graphene dispersion onto a surface of said supporting substrate to form said wet layer of graphene material thereon, drying said wet layer of graphene material to form the dried layer of graphene material, and collecting said dried layer of graphene material deposited on said supporting substrate on a collector roller.

11. The process of claim 10, wherein said dried layer of graphene material isleat treated at first heat treatment temperature prior to said step of collecting said dried layer.

12. The process of claim 3, wherein said second heat treatment temperature includes at least a temperature selected from 100-1,500° C., 1,500-2,500° C., or 2,500-3,200° C.

13. The process of claim 3, wherein said second heat treatment temperature includes a temperature in the range of 300-1,500° C. for at least 1 hour and then a temperature in the range of 1,500-3,200° C. for at least 1 hour.

14. The process of claim 1, wherein said non-carbon elements include an element selected from oxygen, fluorine, chlorine, bromine, iodine, nitrogen, hydrogen, or boron.

15. The process of claim 1, wherein said step (d) of heat treating the dried layer of graphene material at a first heat treatment temperature is conducted under a compressive stress.

16. The process of claim 3, further comprising a compression step to reduce a thickness, a pore size, or a porosity level of said solid graphene foam.

17. The process of claim 1, wherein said graphene dispersion contains a graphene oxide dispersion prepared by

immersing a graphitic material in a powder or fibrous form in an oxidizing liquid in a reaction vessel at a reaction temperature for a length of time sufficient to obtain said graphene dispersion wherein said graphitic material is selected from natural graphite, artificial graphite, meso-phase carbon, meso-phase pitch, meso-carbon micro-bead, soft carbon, hard carbon, coke, carbon fiber, carbon nano-fiber, carbon nano-tube, or a combination thereof and wherein said graphene oxide has an oxygen content no less than 5% by weight.

18. The process of claim **3**, wherein said first and/or second heat treatment temperature contains a temperature in the range of 300° C.-1,500° C. and the graphene foam has an oxygen content or non-carbon content less than 1%, and pore walls having an inter-graphene spacing less than 0.35 nm, a thermal conductivity of at least 250 W/mK per unit of specific gravity, and/or an electrical conductivity no less than 2,500 S/cm per unit of specific gravity.

19. The process of claim **3**, wherein said first and/or second heat treatment temperature contains a temperature in

the range of 1,500° C.-2,500° C. and the graphene foam has an oxygen content or non-carbon content less than 0.01%, pore walls having an inter-graphene spacing less than 0.34 nm, a thermal conductivity of at least 300 W/mK per unit of specific gravity, and/or an electrical conductivity no less than 3,000 S/cm per unit of specific gravity.

20. The process of claim **3**, wherein said first and/or second heat treatment temperature contains a temperature greater than 2,500° C. and the graphene foam has pore walls containing stacked graphene planes having an inter-graphene spacing less than 0.336 nm, a mosaic spread value no greater than 0.4, a thermal conductivity greater than 400 W/mK per unit of specific gravity, and/or an electrical conductivity greater than 4,000 S/cm per unit of specific gravity.

21. The process of claim **1**, further comprising a step of cutting said supercapacitor electrode into multiple sheets of smaller supercapacitor electrode and stacking said multiple sheets to form a thicker electrode for a supercapacitor.

* * * * *